
Specially Funded R&D Program

PCISFRAD Project No. 5

Summary Paper

Design of Spandrel Beams



by

Gary J. Klein

Consultant
Wiss, Janney, Elstner
Associates, Inc.
Northbrook, Illinois

Note: This summary paper is a slightly condensed version of PCISFRAD Project No. 5, "Design of Spandrel Beams." The full report is available from PCI Headquarters at \$8.00 to firms supporting the sponsored research, \$12.00 to PCI Members (non-supporting firms) and \$24.00 to non-PCI Members.

The summary paper, and the full report, are based on a research project supported by the PCI Specially Funded Research and Development (PCISFRAD) Program. The conduct of the

research and the preparation of the final reports for each of the PCISFRAD projects were performed under the general guidance and direction of selected industry Steering Committees. However, it should be recognized that the research conclusions and recommendations are those of the researchers. The results of the research are made available to producers, engineers and others to use with appropriate engineering judgment similar to that applied to any new technical information.

CONTENTS

1. Summary and Conclusions	78
2. Introduction	79
3. Background Research	80
— General Design Considerations	
— Flexure	
— Shear and Torsion	
— Beam End Design	
— Beam Ledges	
— Beam Pockets	
4. Finite Element Model Studies	87
— Spandrel Beam Behavior	
— Transfer of Ledge Loads to Web	
5. Load Tests	91
— Test Specimens	
— Test Procedure	
— Behavior and Strength of Test Specimens	
6. Analysis and Discussion	104
— General Design Considerations	
— Flexure	
— Shear and Torsion	
— Beam End Design	
— Beam Ledges	
— Beam Pockets	
7. Findings and Recommendations	112
Acknowledgments	113
References	114
Appendix A — Notation	115
Appendix B — Spandrel Design Checklist	116
Appendix C — Design Examples	117
— Example 1. L-Beam for Parking Structure	
— Example 2. Pocket Spandrel for Parking Structure	

1. SUMMARY AND CONCLUSIONS

A study of the behavior and design of precast spandrel beams was undertaken. This research project was primarily directed toward spandrel beams commonly used in parking structures. Both L-beams and pocket spandrels were included in the study.

The research included background investigation of design practices, analytical studies using finite element models, and full-scale load tests of two L-beams and one pocket spandrel. All three test specimens were 72 in. high, 8 in. wide and 28 ft long. The target design loads were based on 90 psf dead load and 50 psf live load, which are typical for a double tee parking structure with 60 ft spans.

The background research revealed that industry practices and published procedures vary with respect to several fundamental aspects of spandrel beam design. Behavior near the end regions is not well understood, nor is the influence of connections to deck elements. In general, the design of beam ledges is not consistently handled; in particular, there is no consensus on the design of hanger reinforcement for ledge-to-web attachment. Also, the ACI Building Code (ACI 318-83) does not address combined shear and torsion in prestressed beams. Designers rely on several research reports that give design recommendations.

Ledge-to-web attachment and behavior near the end region of spandrels were identified as the key issues and were the primary focus of this research. The analytical studies and laboratory testing program yielded several significant findings:

- Contrary to several published design examples, a critical section for shear and torsion at the face of the support should be considered.

- Connections to deck elements do not substantially reduce torsion; however, they are effective in restraining

lateral displacement induced by bending about the weak principal axis.

- Shear and torsion design procedures for prestressed spandrels which consider a concrete contribution have been verified by two tests.

- An approach for considering the effect of the pocket on the shear strength of pocket spandrels has been proposed. While the accuracy of this approach has not been fully verified by tests, it is believed to be conservative.

- With regard to detailing practices, it was found that the torsional response of deep spandrels is dominated by out-of-plane bending. The use of lapped-splice stirrups and longitudinal reinforcing bars without hooks does not appear to have any detrimental effect.

- Two independent design checks in the end region of spandrels are recommended. First, reinforcement should be provided to resist out-of-plane bending caused by the horizontal torsional equilibrium reactions. This reinforcement is not additive to the reinforcement for internal torsion. Second, the longitudinal reinforcement in the bearing area should be sufficiently developed to resist the external normal force, in addition to the tension induced by the vertical reaction.

- The eccentricity of the ledge load cannot be neglected in the design of hanger reinforcement for ledge-to-web attachment. Nonetheless, not all of the load acting on the ledge is suspended from the web and the effective eccentricity of the ledge load is significantly reduced due to torsion within the ledge. A design procedure which considers these effects has been recommended. In addition, it was determined that hanger reinforcement is not additive to shear and torsion reinforcement.

- The PCI design equations for punching shear strength of beam ledges may be unconservative. Further research in this area is recommended.

In conclusion, this research has clarified many of the questions relating to spandrel beam design and the design

recommendations will be of immediate benefit to the precast and prestressed concrete industry.

2. INTRODUCTION

Spandrel beams are one of the most complex elements in precast construction. Industry practices and published procedures vary with respect to several fundamental aspects of their design. PCI Specially Funded Research and Development Project No. 5 investigated the behavior and design of precast spandrel beams.

The research program was primarily directed toward deep and slender spandrels such as those commonly used in

parking structures to serve both load-carrying and railing functions. Both L-beams and spandrel beams with pockets for tee stem bearings (pocket spandrels) were included in the program. Fig. 1 shows typical cross sections of these types of beams.

The findings of this research generally apply to both prestressed and nonprestressed spandrels, but may not be applicable to spandrel beams of radically different geometric configuration

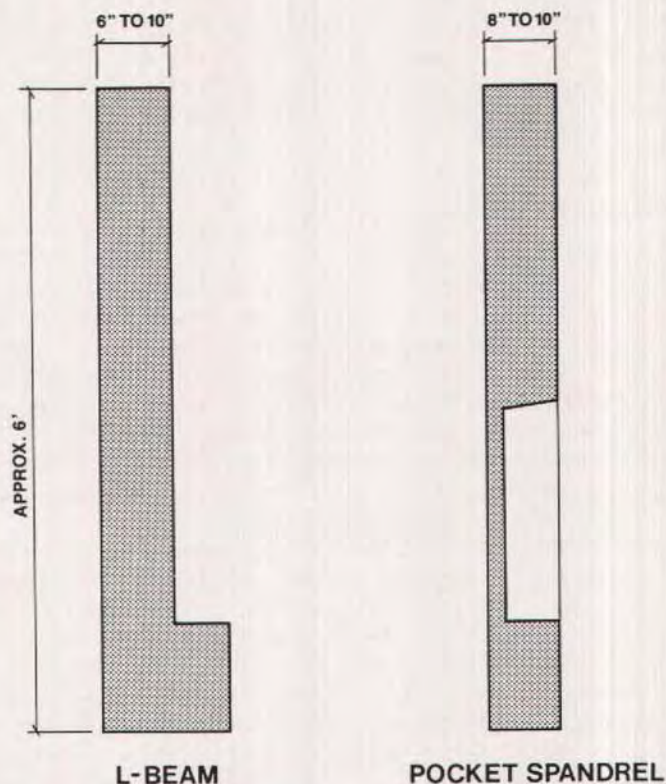


Fig. 1. Typical spandrel sections studied in research program.

or load level. Furthermore, while this research is believed to be reasonably comprehensive, not all aspects of spandrel beam design are covered.

In particular, the research does not address spandrel beam design as part of a lateral load resisting frame, nor the effects of volume change on design and detailing of spandrels. Also, handling and vehicular impact loads are not discussed. These considerations can be very important, but are considered beyond the scope of this research.

The research program included the

following objectives:

- Study of design requirements and practices to determine the state-of-the-art of spandrel beam design.

- Analytical studies using finite element models of an L-beam and pocket spandrel.

- Full-scale tests of two L-beams and one pocket spandrel designed using state-of-the-art methods.

The following sections of this report describe the research, analyze the findings, and provide design recommendations.

3. BACKGROUND RESEARCH

The background research included a review of code requirements, published guides and research reports on spandrel beam design. Questionnaires regarding design methods for L-beams and pocket spandrels were sent to industry designers. The following discussion on spandrel beam design is based on this research.

General Design Considerations

Critical Section — In most precast beams, the loads and reactions are applied at the top and bottom of the beam, respectively. Such beams are said to be "directly loaded." Spandrel beams, on the other hand, are indirectly loaded, and the additional shear capacity due to arch action near the support is not available.¹ Therefore, design for shear and torsion forces at a distance $d(h/2$ for prestressed spandrels) from the support may not be appropriate. Fig. 2 shows potential critical inclined sections which carry all the concentrated loads acting on the ledge rather than just loads farther than d from the support.

The consensus among designers is that all loads acting on the ledge inside the critical section, based on inclined cracking from the edge of the beam base

plate, must be considered as part of the shear/torsion load. This consensus is contrary to the published design examples in Section 4.4 of the PCI Design Handbook² and Example 14.2 in the PCA Notes on ACI 318-83.³ ACI 318-83⁴ does not address indirectly loaded beams; however, Section 11.1.2 of the Commentary recommends special consideration for concentrated loads near supports.

Equivalent Uniform Load — It is common practice to simplify the analysis by replacing concentrated loads with equivalent uniform loads. Some designers increase the equivalent uniform floor load such that the shear and torsion is correct at the critical section at the inside edge of the base plate, i.e., the basic equivalent uniform load is multiplied by the ratio of grid span to design span.

Eccentricity Contributing to Torsion — Typically, the ledge loads are positioned at the centerline of bearing (allowing for volume change and fabrication and erection tolerances) or at the outer one-quarter point of the ledge. The former approach is generally preferred because an increase in ledge projection does not necessarily require an increase in torsional load. The ec-

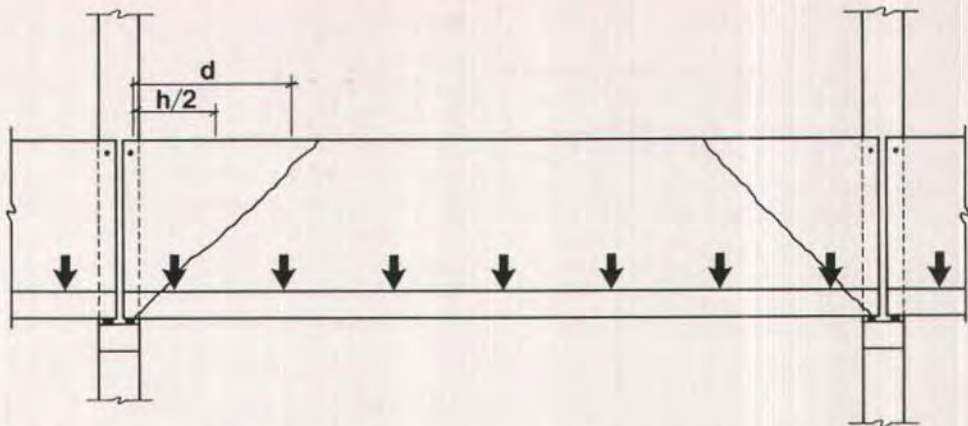


Fig. 2. Inclined failure planes in an "indirectly loaded" spandrel.

centricity contributing to torsion in a spandrel is the distance from the centerline of the web to the applied load, as shown in Fig. 3.

Theoretically, the eccentricity should be measured relative to the shear center, which, for an uncracked L-beam section, is slightly inside the centerline of the web. However, this difference is negligible in deep spandrels. Further, experimental results are not consistent with the theoretical prediction of shear center location based on the uncracked cross section.⁵

Influence of Deck Connections — Prior to connection of the double tees or topping to the spandrels, torsion can be computed as a product of the dead load and the eccentricity between the applied load and centerline of the web. After connections to deck elements are made, however, the applied live load torsion may be partially counteracted by the horizontal force due to friction at the bearing pads coupled with restraint at the deck connections (Fig. 3). However, most practitioners believe that it is inappropriate to rely on a soft bearing pad for this purpose. In addition, recent research⁶ indicates that the effective friction at the bearing pad may be 5 percent or less of the gravity load.

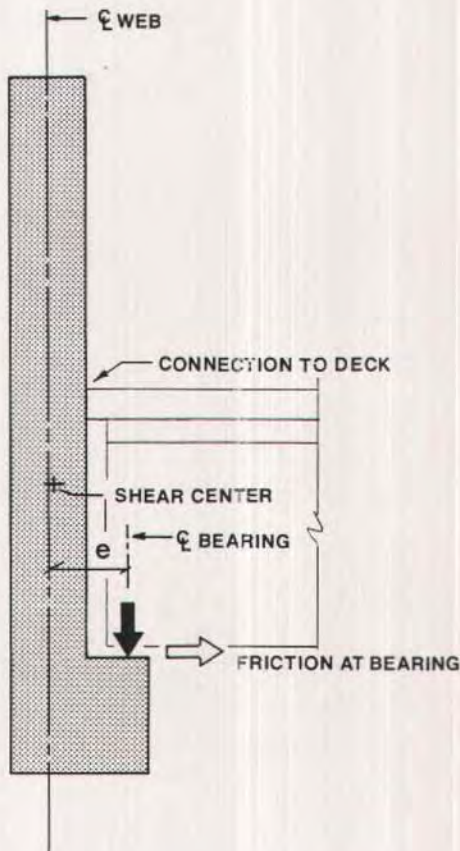


Fig. 3. Eccentricity contributing to torsion in spandrel beam.

Flexure

The flexural design of spandrels generally follows ACI and PCI procedures for bending about the horizontal and vertical axes. However, L-shaped spandrel beams do not have symmetry about either axis. The principal axes are rotated slightly from the vertical and horizontal axes, as shown in Fig. 4. The influence of this rotation on bending about the horizontal axis can be neglected for deep spandrel beams. For shallow spandrels, particularly those employing prestressing, this influence should be considered.

Perhaps more important, however, is

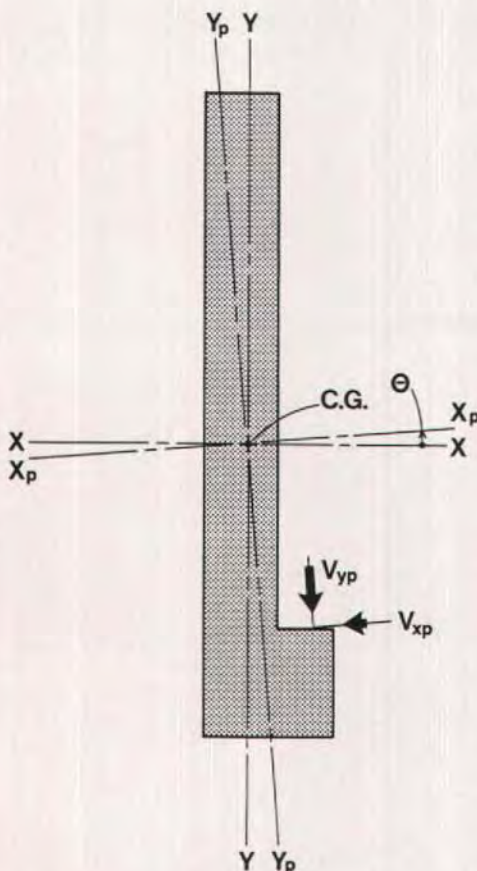


Fig. 4. Principal axes of an L-beam.

the influence of principal axes rotation on horizontal displacement of spandrels. As shown in Fig. 4, a component of the vertical load acts along the weak axis inducing an outward horizontal displacement. All loading prior to making diaphragm connections can cause horizontal displacement. Cleland⁶ found that this was the most dominant behavior of long slender spandrels and suggests a principal axes analysis when the span length is 40 to 50 times the web width, depending on the intermediate support conditions.

In general, detailing practice follows the ACI Code. One noteworthy exception pertains to Section 10.6.7 of ACI 318-83 which is applicable to nonprestressed spandrels. This provision requires that reinforcement be placed in the side faces of webs more than 3 ft deep. The reinforcement is to be distributed in the zone of flexural tension with a spacing not more than the web width, nor 12 in. Designers do not often check this provision; instead, reinforcement in the side faces of the web is designed to resist torsion or handling.

Shear and Torsion

Prestressed Spandrels—The ACI Code does not address torsion in prestressed concrete. A procedure for torsion design of prestressed concrete, which is an extension of the ACI provisions of torsion for nonprestressed concrete, was developed by Zia and McGee.⁷ The second edition of the PCI Design Handbook included a modified version of the Zia and McGee method.⁸ The PCI procedure uses a simplified method for computing torsional stress which is conservative for most spandrel beams.

A further refinement of these methods was subsequently developed by Zia and Hsu.⁹ While the general design approach follows that of Zia-McGee and PCI, new expressions are proposed for torsion/shear interaction and minimum

torsion reinforcement. The Zia-Hsu equations are expressed in terms of forces and moments rather than nominal stresses, which is more consistent with the current ACI Code.

Most designers follow one of these three similar procedures. Practices vary with respect to the design of longitudinal reinforcement for torsion. Some designers consider the prestressing strand to be part of the longitudinal reinforcement while others consider only the mild reinforcing steel. In their original paper, Zia and McGee recommended that only the prestressing steel in excess of that required for flexure, and located around the perimeter of closed stirrups, should be considered as part of the longitudinal torsion steel.

The third edition of the PCI Design Handbook² describes a procedure developed by Collins and Mitchell, which is based on compression field theory. This approach assumes that, after cracking, the concrete can carry no tension and that shear and torsion are carried by a field of diagonal compression. Because the concrete contribution is neglected, this approach will generally require somewhat more stirrup reinforcement depending on the selection of the crack angle. The biggest difference, however, is in the positive and negative moment capacity requirements which are based on the axial tension caused by shear and torsion. For the example shown in the PCI Design Handbook, the required positive and negative bending strength at the face of the support exceeds the midspan moment. These requirements present considerable detailing difficulties, and many designers do not feel they are valid for deep spandrels.

Detailing practices for the torsional reinforcement do not always follow ACI Code requirements. Section 11.6.7.3 requires that transverse reinforcement consist of closed stirrups, closed ties or spirals. However, the Commentary to the ACI Code indicates that this re-

quirement is primarily directed at hollow box sections and solid sections subjected primarily to torsion. In these members, the side cover spalls off, rendering lapped-spliced stirrups ineffective. This type of behavior is unlikely in deep spandrel beams, and transverse reinforcement is often provided by pairs of lapped-spliced U-stirrups. Also, most designers feel that the stirrup spacing limit of 12 in. is not appropriate for deep spandrels, and this limit is routinely exceeded.

Nonprestressed Spandrels — Torsion design of nonprestressed concrete generally follows ACI Code requirements, except for the detailing considerations discussed above.

Pocket Spandrels — Typically, pocket spandrels need not be designed for torsion. However, the pockets complicate the shear design. Design practices vary for considering the effect of the pocket; some designers neglect this effect. Fortunately, shear strength does not control the dimensions of deep pocket spandrels and often only minimum reinforcement is required. Welded wire fabric is frequently used for web reinforcement.

Beam End Design

Torsion Equilibrium — The eccentric load applied on the ledge produces torsion in the spandrel which must be resisted by reactions at the supports. Customarily, the web is connected to the column to restrain rotation. Figs. 5a and 5b show the torsion equilibrium reactions for a normal and dapped connection, respectively.

The torsional equilibrium reactions may require supplemental vertical and horizontal web reinforcement at the ends of the girder. Rath¹⁰ and Osborn* prescribe similar methods for design of

*Osborn, Andrew E. N., "Design of Ledger Girders," Draft Report for PCI Connection Details Committee, April 1984.

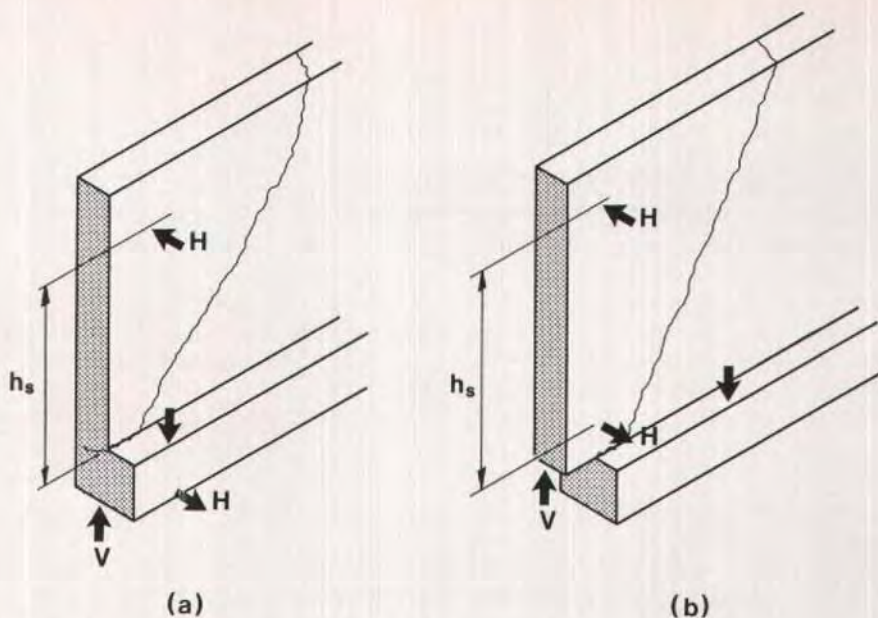


Fig. 5. Torsion equilibrium reactions in spandrel beam.

this reinforcement. Vertical and longitudinal steel, A_{sv} and A_{sl} , on the inside face of the spandrel is calculated by:

$$A_{sv} = A_{sl} = \frac{T_u}{2\phi f_y d_s} \quad (1)$$

where

- T_u = factored torsional moment at end of girder (in.-lbs)
- d_s = depth of A_{sv} and A_{sl} steel from outside face of spandrel (in.)
- f_y = yield strength of reinforcement (psi) (or effective prestress)
- ϕ = strength reduction factor = 0.85

The use of $\phi = 0.85$ instead of 0.90 (flexure) compensates for the ratio of internal moment to total effective depth, which is not in Eq. (1).

Osborn recommends the bars be evenly distributed over a height and width equal to h_s (see Fig. 5) from the concentrated reaction point.

Because shear cracks may coincide with diagonal cracks due to out-of-plane bending, A_{sv} should be added to the

shear reinforcement. However, most designers feel this reinforcement is not additive to reinforcement for internal torsion. If the reinforcement for torsion is considered to function as A_{sv} and A_{sl} reinforcement, little or no supplemental reinforcement is required provided all loads acting on the ledge are considered as part of the shear/torsion load.

Fig. 6 shows an alternative means to provide torsional equilibrium at the support. In this case, the end reactions are in close alignment with the ledge loads. The projecting beam ledge is treated as an upside-down corbel. Most designers surveyed indicated that this approach may lead to excessive rolling of the spandrel beam at the support, particularly where a soft bearing pad is used.

Dapped-End Beams — Section 6.13 of the PCI Design Handbook presents design criteria for dapped-end connections. Research on dapped connections under PCISFRAD Project No. 6, which is being conducted concurrently with

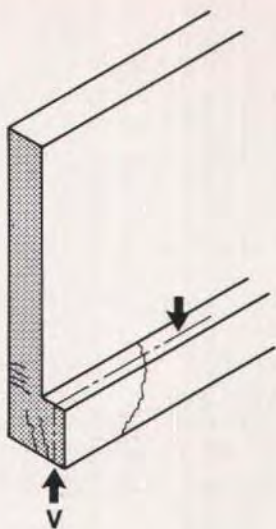


Fig. 6. Beam end corbel behavior when providing torsion equilibrium at support of spandrel beam.

this project, is expected to recommend modified procedures. Design of dapped-end L-beams is often complicated by reinforcement for torsion equilibrium connections (Fig. 5b). Also, the last breakout in a pocket spandrel often interferes with the reinforcing for the dapped end. The established design procedures are modified as appropriate to handle these special conditions.

Beam Ledges

Hanger Reinforcing — Fig. 7 illustrates a possible separation between the ledge and web of an L-shaped spandrel. Section 6.14 of the PCI Design Handbook and design examples by PCA³ and Collins and Mitchell¹¹ recommend hanger reinforcement concentrated near the ledge load given by:

$$A_{sh} = \frac{V_u}{\phi f_y} \quad (2)$$

The notation is defined on the next column above.

Raths¹⁰ uses all the hanger reinforcement between ledge loads, but computes the required reinforcement based on the summation of moments about the outside face of the spandrel, thus:

$$A_{sh} = \frac{V_u}{\phi f_y} \frac{(jd + a)}{jd} \quad (3)$$

where

A_{sh} = area of transverse hanger reinforcement on inside face of spandrel for each ledge load (sq in.)

V_u = factored ledge load (kips)

a = distance from ledge load to center of inside face reinforcement (in.)

jd = internal moment arm (in.) (taken as $d - \frac{1}{2}$ in.)

ϕ = strength reduction factor = 0.85

Raths recommends an additional load factor of 4/3 for design of hanger rein-

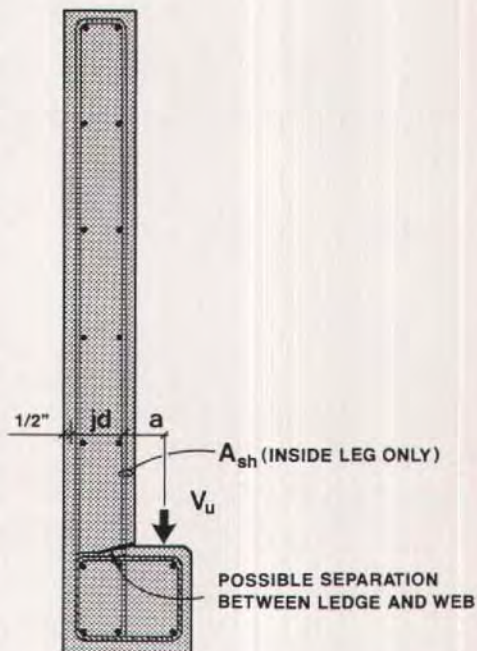


Fig. 7. Ledge-to-web attachment showing hanger reinforcing.

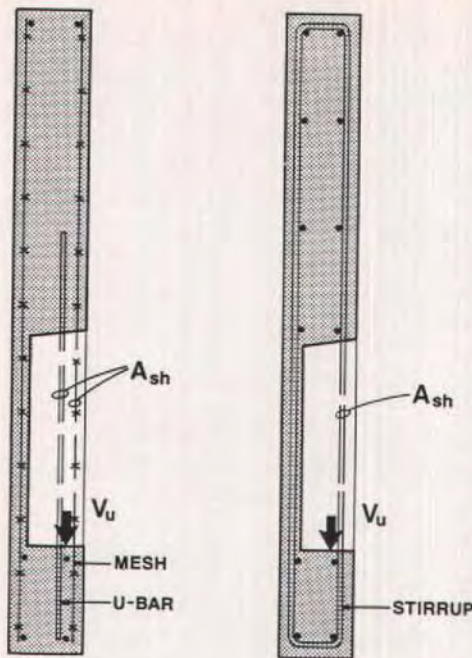


Fig. 8. Hanger reinforcement in pocket spandrels.

forcement. An alternate procedure for using concrete tension as a means of ledge-to-web attachment is also given in his paper.

Eq. (3) is based on sound principles of statics, yet there are many existing spandrels that have performed well with much less reinforcement than this equation would require. The only known failures have occurred where there was no hanger reinforcement. In several instances, beams with very light hanger reinforcement have survived loading tests.

Further refinements of hanger reinforcement design^{11,*†} reduce the load that must be suspended from the web

*Osborn, Andrew E. N., "Design of Ledger Girders," Draft Report for PCI Connection Details Committee, April 1984.

†Sturm, Edward R., "Theory of Deflection Compatibility," Private correspondence with Andrew Osborn, May 1984.

based on internal shear stress distribution, relative depth of the ledge, and deflection compatibility.

There is no consensus among designers on requirements for hanger reinforcement. Some designers do not check ledge-to-web attachment, while others use some combination of the above methods. Furthermore, there is no agreement as to whether or not hanger reinforcement should be added to shear and torsion reinforcement. The method for designing hanger reinforcement generally controls the quantity of transverse reinforcement in the middle region of the spandrel, and can have a very significant effect on material and fabrication costs.

Ledge Punching Shear — The design for punching shear in beam ledges generally follows the procedures in Section 6.14 of the PCI Design Handbook. Some designers follow a modified procedure recommended by Raths;¹⁰ based on unpublished test results, this method considers a lower ultimate stress on the vertical shear plane along the inside face of the web. Mirza, et al^{12,13} and Krauklis and Guedelhofer¹⁴ have also found that the PCI design equations may be unconservative.

Beam Pockets

It is customary to provide closed stirrups or U-bars in the plane of the web for the entire tee stem load in pocket spandrels. The hanger bars are typically located near the tee stem reaction, as shown in Fig. 8. Therefore, Eq. (2) is used to determine hanger reinforcement requirements. The concrete tensile stress at the reaction level is relatively low so a horizontal crack at that location is unlikely. Also, because hanger reinforcement is customarily used, punching shear below the pocket is generally not a concern.

Prior to describing the experimental program, a summary of the finite element model studies is given.

4. FINITE ELEMENT MODEL STUDIES

Description

Finite element models of an L-beam and pocket spandrel were analyzed. The geometry of these models and the test specimens was essentially the same. Refer to Figs. 13 and 14 for more detailed information on the geometry of the beams.

The model studies had several objectives:

- Investigate the deflections and rotations caused by the eccentrically applied load.

- Determine the theoretical torsional equilibrium reactions at the supports.

- Study the influence of connections to deck elements on deformations and torsional equilibrium reactions.

- Investigate the stresses across the ledge/web interface.

Three-dimensional solid elements were used with three degrees of freedom at each node. Cross sections showing the finite element mesh are shown in Figs. 9 and 10.

Service loads included beam dead load and a 16.8 kip tee stem reaction at 4 ft centers. The tee stem load was applied at 8 in. and 2 in. from the web centerline for the L-beam and pocket spandrel, respectively. The restraints at each end of the beam modeled a typical spandrel beam support where the bearing pad is placed at the centerline of the web, and lateral support is provided near the bearing and at the top corners of the beam.

For both the L-beam and pocket spandrel, a second condition was analyzed in which additional lateral restraint was provided near midheight of the beam to simulate connections to deck elements. There was no possibility of relative lateral movement between the column restraints and deck elements, simulating the case where there is an independent connection between the deck and the column. This case was

considered so the analytical studies and load tests modeled the same condition, although it should be noted that a direct connection between the column and deck is not necessarily required. Alternately, the column can be indirectly connected to the deck through the spandrel beam.

Spandrel Beam Behavior

Fig. 9a shows the midspan deflection of the L-beam at service load without any connections to deck elements. Note the overall outward deflection due to the rotation of the principal axes. Connections to deck elements effectively restrain this outward displacement, as shown in Fig. 9b. Usually these connections are not made until all of the dead load is in place. Similar plots for the pocket spandrel are shown in Fig. 10. Due to the different cross-sectional shape and load eccentricity, the lateral deflection is relatively small.

Fig. 11a shows the horizontal reactions at the L-beam support without connections between the spandrel and deck. These forces simply balance the external torsion due to the eccentrically applied loads. Fig. 11b shows the horizontal reactions with deck connections. The deck connections in the midspan region restrain the outward displacement. The deck connections at the support work with the top corner connections to restrain rotation. The net outward force between the deck and spandrel would be counteracted by the column-to-deck connection. If there were no column-to-deck connection, the deck connection forces would tend to balance, depending on the stiffness of the column.

Transfer of Ledge Loads to Web

Stresses across a plane 3 in. above the ledge/web interface were studied. (The

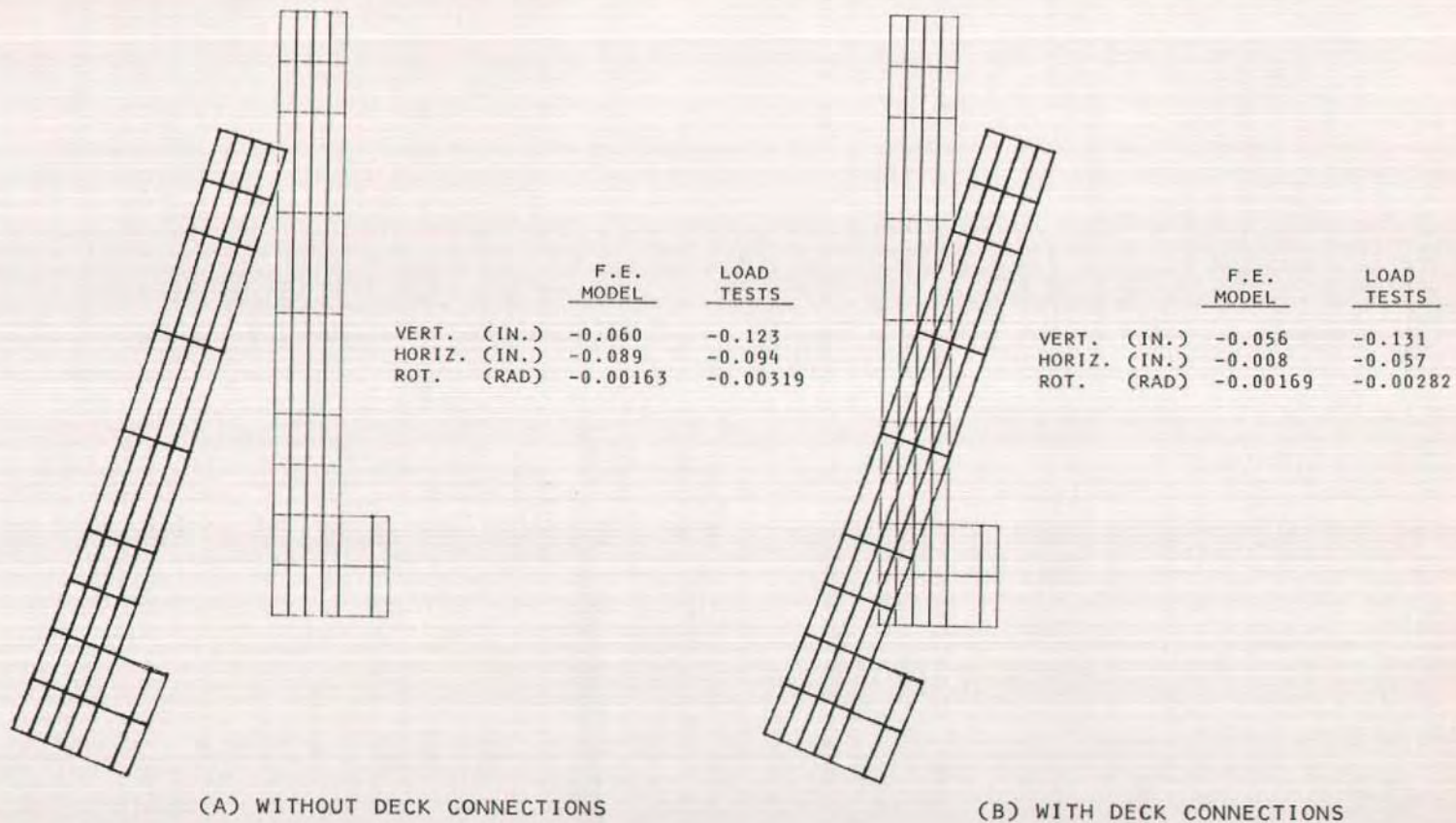
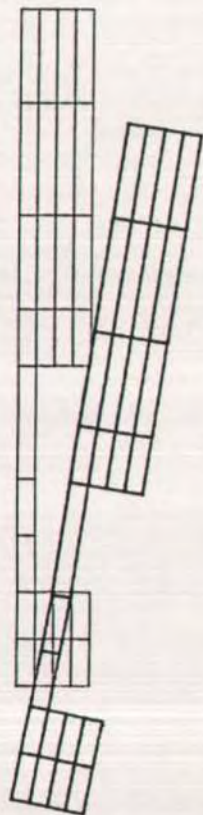


Fig. 9. Midspan deflection of L-beam (superimposed dead load plus live load).



	<u>F. E. MODEL</u>	<u>LOAD TESTS</u>
VERT. (IN.)	-0.053	-0.173
HORIZ. (IN.)	+0.024	+0.038
ROT. (RAD)	-0.00085	-0.00443

(A) WITHOUT DECK CONNECTIONS



	<u>F. E. MODEL</u>	<u>LOAD TESTS</u>
VERT. (IN.)	-0.053	-0.146
HORIZ. (IN.)	0.0	+0.013
ROT. (RAD)	-0.00083	-0.00346

(B) WITH DECK CONNECTIONS

Fig. 10. Midspan deflection of pocket spandrel (superimposed dead load plus live load).

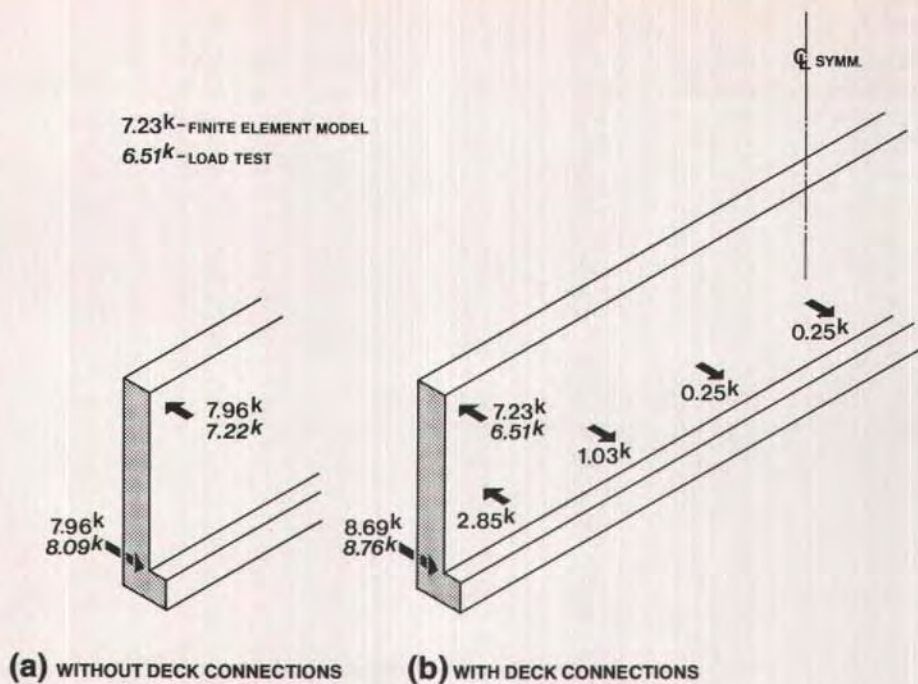


Fig. 11. Horizontal forces acting on L-beam.

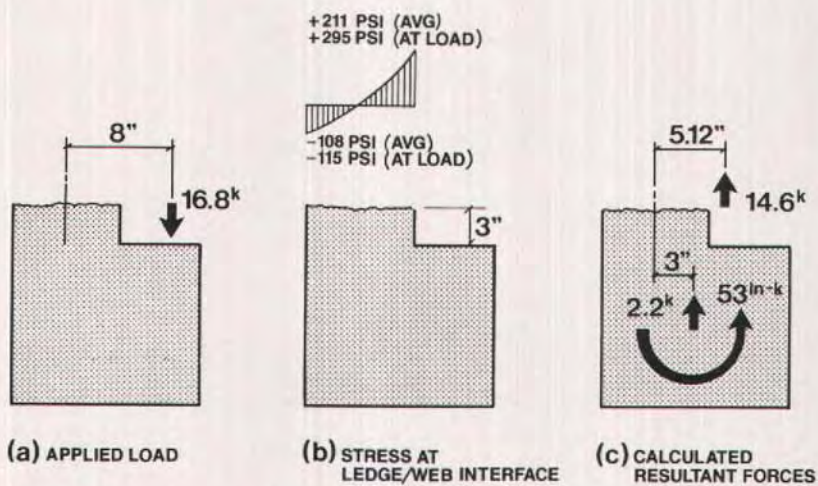


Fig. 12. Study of ledge region from finite element model.

geometry of the finite element mesh prevented investigation at the top of the ledge.) The results of that study are presented in Fig. 12. As expected, the inside face of the web is in tension. The maximum tensile stress of 295 psi, which occurs at the ledge load, is about 40 percent greater than the average stress. The compression in the outside face of the web is significantly more uniform.

The resultant of these stresses can be computed by integrating stresses in the individual elements near the ledge/web junction. As indicated in the figure, the resultant is slightly less than the applied ledge load and is shifted significantly towards the web centerline. These differences are equilibrated by shear and torsion in the ledge itself. This mechanism is described in more detail in Section 6.

5. LOAD TESTS

Two L-beams and one pocket spandrel were tested to study their behavior and verify their strength. The tests were conducted in the structural laboratory of Wiss, Janney, Elstner Associates in Northbrook, Illinois.

Test Specimens

General — All three spandrels were 72 in. high, 8 in. wide and 28 ft long. The target design loads were based on 90 psf dead load and 50 psf live load, which are typical for a double tee parking structure with 60 ft spans. The reactions at each stem of an 8 ft wide double tee were 16.8 kips.

Design — The design of the test specimens was based on the state-of-the-art methods described in the background section. Shear and torsion design for the prestressed spandrels followed the procedure recommended by Zia and Hsu. ACI Eq.(11-10) [rather than Eq.(11-11) or (11-13)] was used to compute the basic shear strength provided by the concrete section. Flexural design followed ACI 318-83. Some reserve flexural strength was required to meet the provisions of Section 18.8.3, which requires a bending capacity equal to at least 1.2 times the cracking moment. Reinforcement for torsional equilibrium was checked by Eq.(1). This reinforcement was not added to the reinforcement

for internal torsion.

In view of the controversy regarding ledge-to-web attachment, alternate procedures were used for design of hanger reinforcement:

- Hanger reinforcement for Specimen 1 was designed by Eq.(2), with a one-sixth reduction in the load suspended from the web based on relative ledge depth. All of the transverse reinforcement between ledge loads was considered to be effective, and hanger reinforcement was not added to shear and torsion reinforcement.

- Eq.(3) was used for design of the hanger reinforcement in Specimen 2. A 7.4 percent reduction in the suspended load was taken based on an assumed parabolic shear stress distribution. Again, all the hanger reinforcement between ledge loads was considered effective, and it was not added to shear/torsion reinforcement.

Hanger reinforcement for the pocket spandrel (Specimen 3) was designed by Eq.(2). In addition to a U-bar at the pocket, one wire on each side of the pocket from the mesh reinforcing was considered to contribute.

Design of the dapped-end connection for the pocket spandrel basically followed the PCI Design Handbook procedure with two exceptions. First, due to relatively low stresses, there was no special reinforcement provided for di-

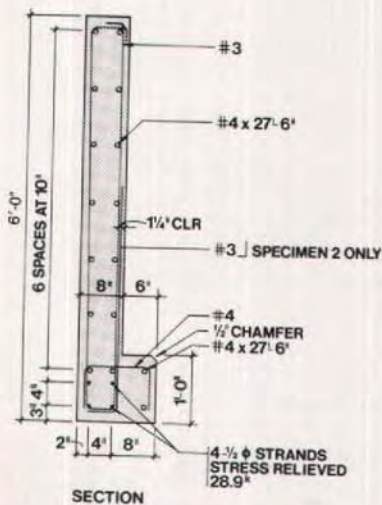
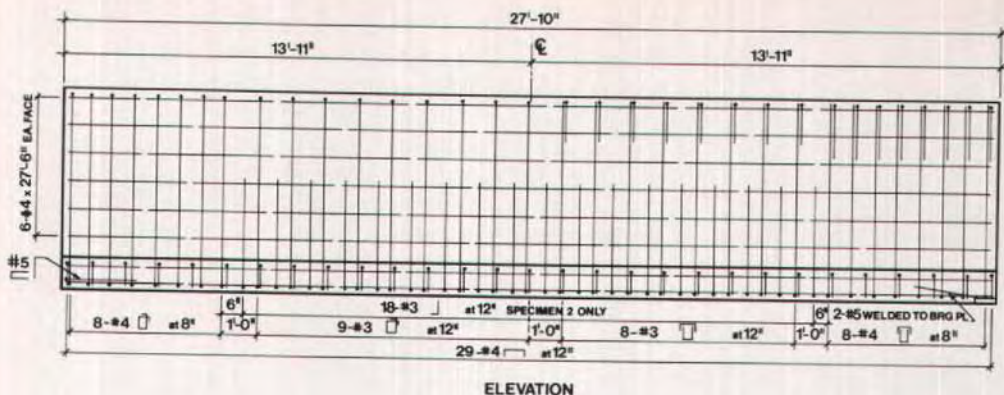


Fig. 13. Dimensions and details of Specimens 1 and 2.

agonal tension in the extended end or direct shear at the junction of the dap and the main body of the member. The welded wire shear reinforcement, however, was continued into the extended end. Second, the reinforcement for flexure and axial tension in the extended end was not continued past the potential diagonal tension crack extending to the bottom corner of the beam.

Details — The dimensions and reinforcement details of the test specimens

are provided in Figs. 13 and 14. The following features of the reinforcing details should be noted:

- Due to the different design methods, Specimen 2 has twice as much hanger reinforcement across the ledge-web interface. This reinforcement was provided by partial height L-bars on the inside face of the spandrel between the stirrups. These bars add about 4 percent to the weight of the mild steel in the beam.

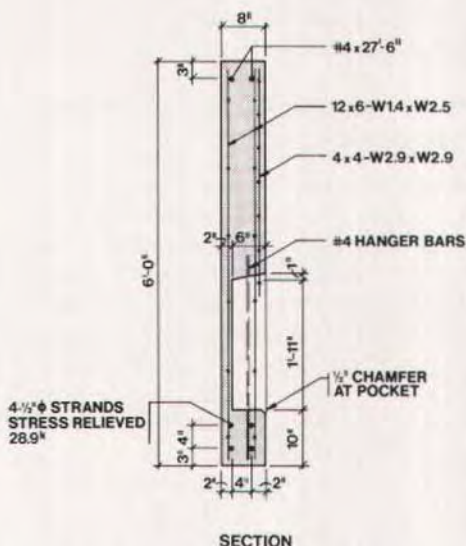
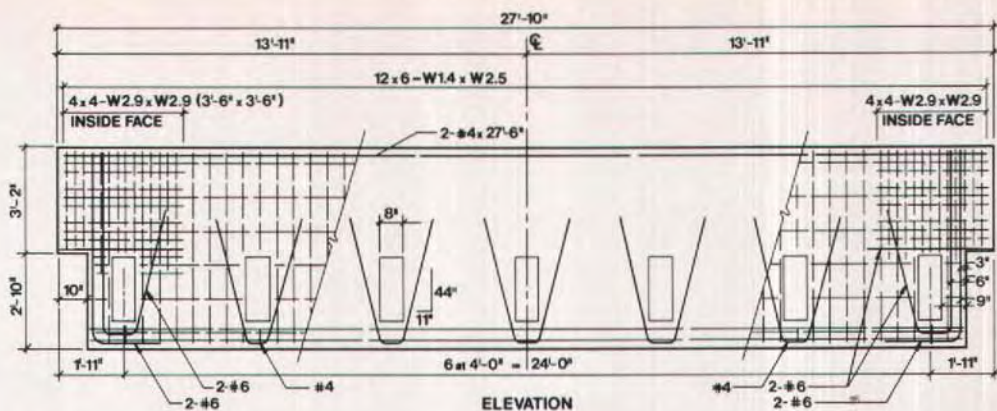


Fig. 14. Dimensions and details of Specimen 3.

● Closed ties formed in one piece by overlapping 90 degree end hooks are used on the left half of the L-beams. Stirrups on the right side of the L-beams consist of lapped-spliced U-bars.

● The longitudinal bars in the L-beams are not hooked at the ends.

● At the right side of the L-beams, two #5 bars are welded to a bearing plate. A #5 U-bar is used on the left side of the L-beams.

● Wire mesh is used for shear rein-

forcement of the pocket spandrel. The mesh is not hooked around the main reinforcement at the top and bottom of the beam, although the ACI Code requirements for development of web reinforcement (Section 12.13.2.5) are satisfied.

Materials — Design of the test specimens was based on 5000 psi concrete, 60 ksi reinforcing bars (ASTM A706), 270 ksi stress-relieved strand, and ASTM A497 mesh. Concrete cylinders and re-

Table 1. Material strengths.

Concrete		Reinforcing steel		
Specimen	Compressive strength f'_c (psi) ^(a)	Bar size	Yield strength f_y (ksi)	Tensile strength f_u (ksi)
1	5330	#3	78.9	98.7
2	5640	#4	70.4	103.7
3	6060	#6	64.2	98.1

(a) Average of three field-cured cylinders tested concurrently with load test (psi).

inforcing bar samples were tested to determine actual strengths. The results are presented in Table 1. The yield strength of the #3 bars was much higher than expected.

Test Procedure

Setup — The test setup is shown in Fig. 15. The spandrels were supported on rigid L-shaped frames which provided lateral restraint at the four corners of the beam. Load was applied at seven points along the beam using specially designed double tees (and one single tee). The test setup featured a removable connection between the spandrels and double tees.

Instrumentation — Instrumentation included load cells at two of the loading points on the double tees, as well as all four horizontal reaction points. Three deflection transducers and one tiltmeter were set up at midspan to monitor horizontal and vertical deflections and rotations. Finally, single element strain gauges were placed on selected reinforcing bars as per Table 3.

Load sequence — Initially, each spandrel was incrementally loaded to service load (16.8 kips per tee stem) without the connection between the double tees and spandrels. After unloading, this sequence was repeated with the deck connections in place. Finally, the beams were loaded to failure without the deck connections in increments of 2.5 kips per tee stem. The third specimen was

tested to failure in two phases. After a failure near the end region in Phase 1, the supports were moved in 4 ft from each end, and the specimen was reloaded to failure.

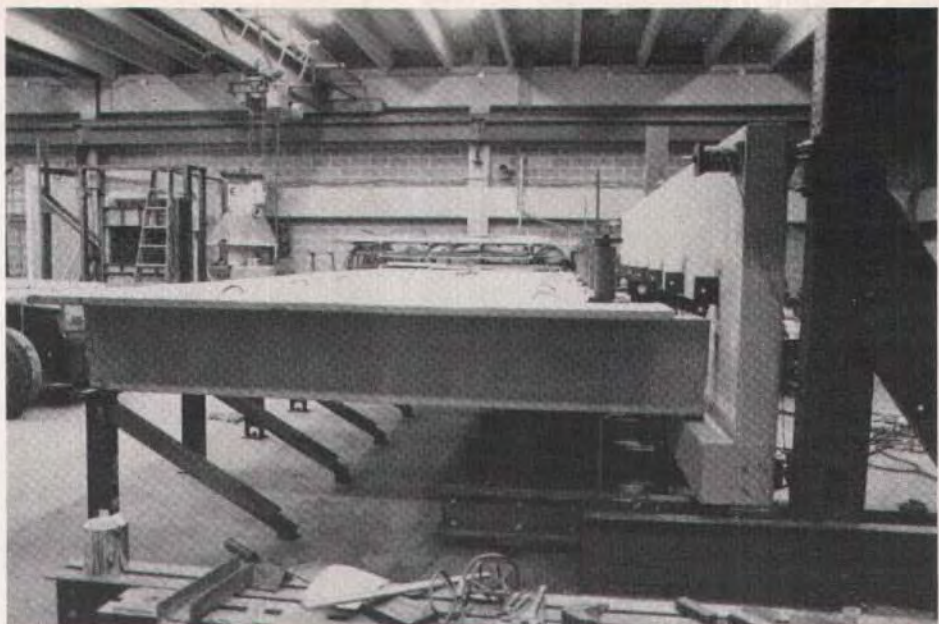
Behavior and Strength of Test Specimens

Deflection and Rotation — Figs. 9 and 10 compare the measured deflections of the L-beam and pocket spandrel to those predicted by the finite element models. Although the measured deflections are quite small, they are two to three times the predicted deflections. About half of the vertical deflection and some of the rotation may be attributed to deformation of the bearing pads.

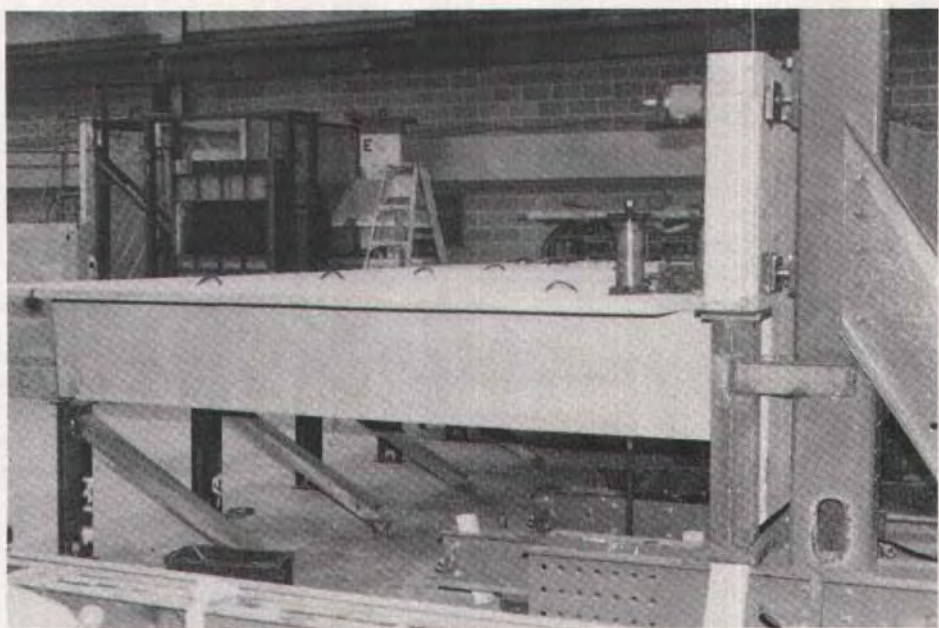
Fig. 16 shows a plot of stem reaction vs. midspan torsional rotation of Specimen 2. The stiffness of the beam is significantly reduced after cracking was observed.

Service Load Behavior — At service load, no cracks were observed in the L-beams. However, minor cracks were observed near the dapped-end connection of the pocket spandrel. These cracks, which are shown in Fig. 17a, were all less than 10 mils (0.010 in.) in width.

Failure Patterns (Specimen 1) — The cracking patterns that occurred during loading to failure are shown in Fig. 18a. Diagonal cracks began to appear on Specimen 1 at a load of 25 kips per stem. The crack at the ledge/web junction oc-



(a) L-beams



(b) Pocket spandrel

Fig. 15. Test setup for L-beams and pocket spandrel.

Table 2. Spandrel design and test results.

Failure mechanism	Units	Specimen No. ^a	Design force		ϕ	Calculated strength		Test force ^d
			Service	Ultimate		Design ^b ($\phi \times$ Nominal)	Predicted ^c $\phi = 1$	
Midspan flexure	in.-kips	1	5,490	8,190	0.90	11,900 ^f	13,730	10,520
		2	5,490	8,190	0.90	11,900 ^f	13,730	12,800
		3-1	5,410	8,080	0.90	9,400 ^f	10,440	8,150
Shear at support	kips	1	<u>68.0</u>	<u>101.4</u>	0.85	<u>111.1</u>	<u>145.2</u>	<u>130.3</u>
Torsion at support	in.-kips	2	<u>470</u>	<u>709</u>		<u>793</u>	<u>1033</u>	<u>967</u>
			<u>68.0</u>	<u>101.4</u>	0.85	<u>111.1</u>	<u>146.8</u>	<u>158.6</u>
		3-1	<u>470</u>	<u>709</u>		<u>793</u>	<u>1033</u>	<u>1196</u>
			<u>66.9</u>	<u>100.0</u>	0.85	<u>124.7</u>	<u>159.0</u>	<u>100.9</u>
		3-2	<u>118</u>	<u>177</u>		<u>e</u>	<u>e</u>	<u>186</u>
			<u>66.9</u>	<u>100.0</u>	0.85	<u>124.7</u>	<u>159.0</u>	<u>124.7</u>
			<u>118</u>	<u>117</u>		<u>e</u>	<u>e</u>	<u>238</u>
Lateral bending due to torsion equilibrium force	in.-kips	1	470	709	0.90	692	902	967
		2	470	709	0.90	692	902	1196
		3-1	118	177	0.90	246	273	186
Hanger reinforcement at dapped end	kips	3-1	66.9	100.0	0.90	95.0	113.0	100.9
Hanger reinforcement for ledge load	kips per stem	1	16.8	25.3	0.90	28.4 ^e	41.5 ^e	34.6 ^h
		2	16.8	25.3	0.90	26.8 ^h	39.1 ^h	42.7
		3-2	16.8	25.3	0.90	24.1 ^j	30.8 ^j	47.6


Table 2 (cont.). Spandrel design and test results.

Failure mechanism	Units	Specimen No. ^a	Design force		ϕ	Calculated strength		Test force ^d
			Service	Ultimate		Design ^b ($\phi \times$ Nominal)	Predicted ^c $\phi = 1$	
Tee stem bearing ^l	kips per stem	1	16.8	25.3	0.70	66.8	101.7	34.6
		2	16.8	25.3	0.70	66.8	107.6	42.7
		3-2	16.8	25.3	0.70	66.8	115.6	47.6
Ledge punching shear at interior bearing ^m	kips per stem	1	16.8	25.3	0.85	61.7	74.9	34.6
		2	16.8	25.3	0.85	61.7	77.1	42.7
Ledge punching shear at exterior bearing ⁿ	kips per stem	1	16.8	25.3	0.85	53.7	65.2	34.6
		2	16.8	25.3	0.85	53.7	67.1	42.7

^a 3-1 and 3-2 indicate Phases 1 and 2 of the Specimen 3 load test, respectively.

^b Calculated nominal strength using state-of-the-art design equations and specified material properties (multiplied by ϕ).

^c Calculated nominal strength using design equations and actual material properties ($\phi = 1$).

^d  indicates failure at specified test force.

^e Torsion design not required.

^f Reserve flexural strength was required to meet the requirements of Section 18.8.3 of ACI 318-83 which requires a bending capacity equal to at least 1.2 times the cracking moment.

^g Hanger reinforcement designed by Eq. (2) with a one-sixth reduction in the load suspended from the web based on relative ledge depth.

^h Hanger reinforcement designed by Eq. (3) with a 7.4 percent reduction in the load suspended from the web based on parabolic shear stress distribution.

ⁱ Hanger reinforcement designed by Eq. (2); one wire on each side of pocket included.

^k Hanger reinforcement yield at 29.9 kips per stem.

^l Bearing design per PCI Eq. (6.8.1) with $N_u = 0$.

^m Using PCI Eq. (6.14.1).

ⁿ Using PCI Eq. (6.14.2).

Table 3. Reinforcement strains.

Location	Gage No. ^a	Distance from load (in.)	Service load		Factored load		Max test load	
			Load ^b	Strain percent	Load ^b	Strain percent	Load ^b	Strain percent
Ledge hanger reinforcement (near midspan)	1-1	0	16.9	0.004	27.3	0.239	34.6	^c
	1-2	12	16.9	0.001	27.4	0.120	35.6	3.211
	1-3	24	16.9	0.0	27.4	0.223	34.6	2.235
	1-4	12	16.9	0.0	27.4	0.245	34.6	^c
	1-5	0	16.9	0.003	27.4	^c	34.6	^c
Ledge flexure reinforcement	1-6	24	16.9	-0.002	27.4	0.016	34.6	0.015
	1-7	0	16.9	-0.001	27.4	0.026	34.6	0.042
Ledge hanger reinforcement (near midspan)	2-1	24	16.7	0.0	28.1	0.005	42.7	^c
	2-2	18	16.7	0.001	28.1	0.007	42.7	0.210
	2-3 ^c	12						
	2-4	6	16.7	0.002	28.1	0.023	42.7	0.412
	2-5	0	16.7	0.004	28.1	0.035	42.7	^c
Ledge flexure reinforcement	2-6	24	16.7	-0.002	28.1	-0.003	42.7	0.016
	2-7	0	16.7	-0.001	28.1	0.007	42.7	0.034
Dapped end flexure reinforcement	3-1	8	16.7	0.056	24.9	0.130	—	—
Dapped end hanger reinforcement	3-2	8	16.7	0.091	24.9	0.097	—	—
	3-3	11	16.7	0.017	24.9	0.067	—	—
Hanger reinforcement at pocket (at midspan)	3-4	6	16.7	0.006	24.9	0.101	46.8	0.414
	3-5	6	16.7	0.005	24.9	0.093	46.8	0.162

^a First number indicates specimen number.

^b Average ledge load (kips).

^c Bad readings due to gauge failure or bending in bar at crack.

occurred at 27.5 kips. This crack immediately opened to 20 mils and extended end to end where it connected to inclined cracks in the ledge. The ledge continued to separate from the web until the test was stopped at a ledge load of 34.6 kips per stem. At the end of the test, the crack at the ledge/web junction was over 1/8 in. wide, as shown in Fig. 19.

Failure Patterns (Specimen 2) — As shown in Fig. 18b, a well developed pattern of inclined and "rainbow" cracking developed on the inside face of Specimen 2. Typically, these cracks were less than 10 mils wide. Also, several 1 to 3 mil flexural cracks were ob-

served on the outside face. The crack at the ledge/web junction was restrained by the additional hanger reinforcement, as shown in Fig. 20. At a load of 42.7 kips per tee stem, punching shear failures occurred at the first and sixth tee stem from the left. Fig. 21 shows the punching shear failures. The failure cone initiates behind the bearing pad. The failure surface is almost vertical near the top and inclined below the ledge reinforcing. As a result, the ledge flexural reinforcement is not very well developed across the failure plane.

Failure Patterns (Specimen 3) — The cracks which formed during Phase 1 of

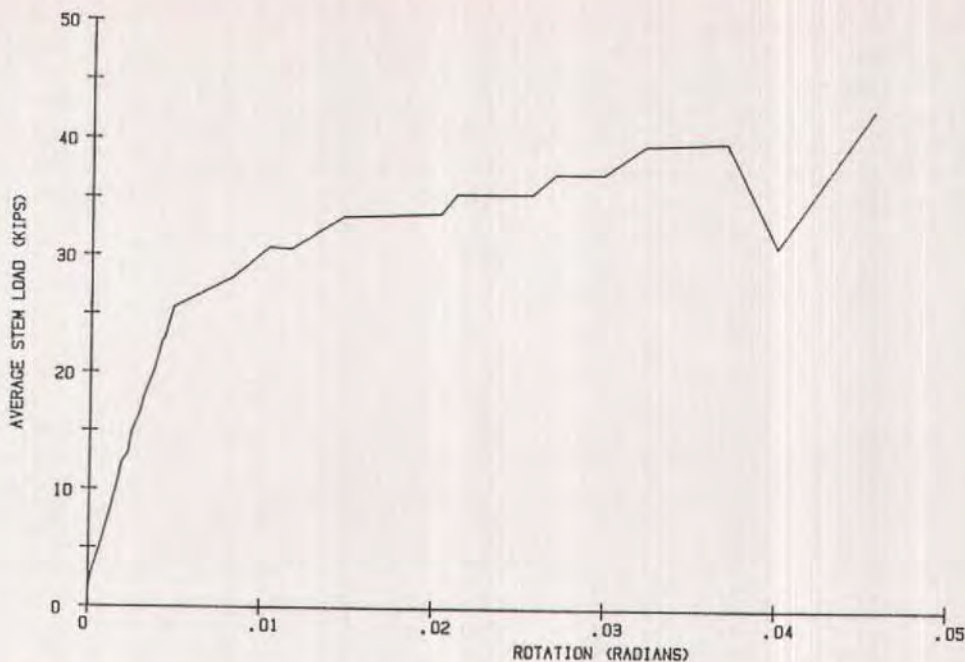


Fig. 16. Stem reaction versus rotation (Specimen 2).

the Specimen 3 test are shown in Fig. 17b. Cracks near the dapped-end connection which developed at service load continued to lengthen and widen, and new inclined cracks formed. Cracks below the pockets began to form at tee stem loads of 18 to 25 kips. As the load was increased, diagonal tension cracks developed further from the support. These cracks typically initiated near midheight of the beam. At a load of 26.5 kips per tee stem, a diagonal tension crack near the right support extended down to the bottom corner of the beam and failure occurred immediately, as shown in Fig. 22.

In Phase 2 of the Specimen 3 test, a wide "rainbow" crack formed at a load of about 43 kips per tee stem. Apparently this crack is due to a combination of diagonal tension due to shear and vertical tension due to the tee stem loads. The ultimate failure, however, occurred when the concrete below the fifth pocket from the left punched out at

47.6 kips. The "rainbow" crack and punching failure are shown in Fig. 17c.

Strength — Table 2 summarizes the design force, calculated strength and test force for several potential and actual failure mechanisms. The calculated strengths are based on the equations used for design. Because the hanger reinforcement for Specimens 1 and 2 was designed using different equations, the calculated strength is roughly the same even though Specimen 2 had twice as much hanger reinforcement.

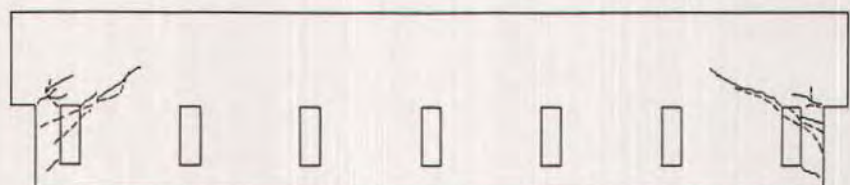
The calculated strength is expressed as both a "design" strength and a "predicted" strength. The design strength is based on specified material properties, and includes the appropriate strength reduction factor. The predicted strength uses actual material properties and no strength reduction factor.

As shown in Table 2, the spandrel beams were tested to a load near or beyond their predicted capacity for several of the primary failure mechanisms.

There were, however, several notable exceptions.

The shear failure of Specimen 3 (Phase 1) occurred at the diagonal cracking load, and the expected contribution from the shear reinforcing was not realized.

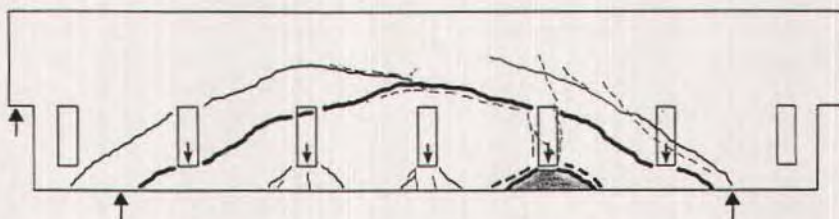
The ledge-to-web attachment strength of Specimen 1 was considerably less than predicted by Eq.(2). In contrast, Specimen 2 showed no sign of a ledge-to-web attachment failure, even though the test force was slightly above the capacity predicted by Eq.(3). The strength



(A) FRONT ELEVATION OF SPECIMEN 3
AT SERVICE LOAD



(B) FRONT ELEVATION OF SPECIMEN 3-(PHASE 1)
AT ULTIMATE LOAD



(C) FRONT ELEVATION OF SPECIMEN 3-(PHASE 2)
AT ULTIMATE LOAD (END REGION CRACKS NOT SHOWN)

- CRACK LEGEND:
- 1-10 MIL
 - 11-49 MIL
 - 50 MIL OR MORE
 - CRACK ON BACK (OUTSIDE) FACE

Fig. 17. Crack patterns (Specimen 3).

of the hanger reinforcement below the pocket of Specimen 3 (Phase 2) was well beyond the predicted capacity. Apparently, the shear strength of the concrete below the pocket contributed.

The most surprising result was the punching shear failure at Specimen 2. Although the ledge loads were quite high, the punching shear strength was only about 60 percent of the predicted capacity.

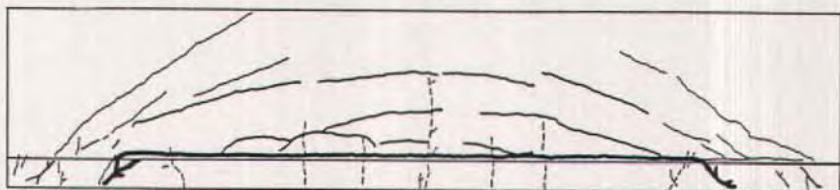
Horizontal Reactions — At service loads, the measured horizontal reactions at the supports were comparable to the reactions predicted by the finite element model, as shown in Fig. 11.

Reinforcement Strain — Table 3 summarizes the reinforcement strain at gauged locations. Data are provided at

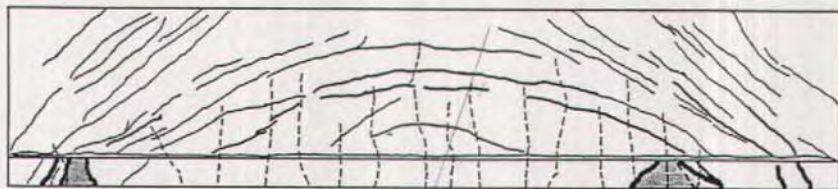
or near service load, factored load and the maximum test load.

At service load reinforcement, strains are insignificant except at the dapped-end connection of the pocket spandrel, where the strain in the hanger reinforcement bar nearest the load is almost 0.1 percent. This strain level corresponds to half the yield stress for a Grade 60 bar. Even though the strain levels in the ledge flexure and hanger reinforcing are very low, they are noticeably higher at the ledge load.

At factored load, cracking of the ledge/web junction of Specimen 1 was accompanied by very high hanger reinforcement strain. In Specimen 2, this cracking was limited to the vicinity of the ledge load which is reflected in the



(A) FRONT ELEVATION OF SPECIMEN 1
AT ULTIMATE LOAD



(B) FRONT ELEVATION OF SPECIMEN 2
AT ULTIMATE LOAD

CRACK LEGEND:

- 1-10 MIL
- 11-49 MIL
- 50 MIL OR MORE
- CRACK ON BACK (OUTSIDE) FACE

Fig. 18: Crack patterns (Specimens 1 and 2).

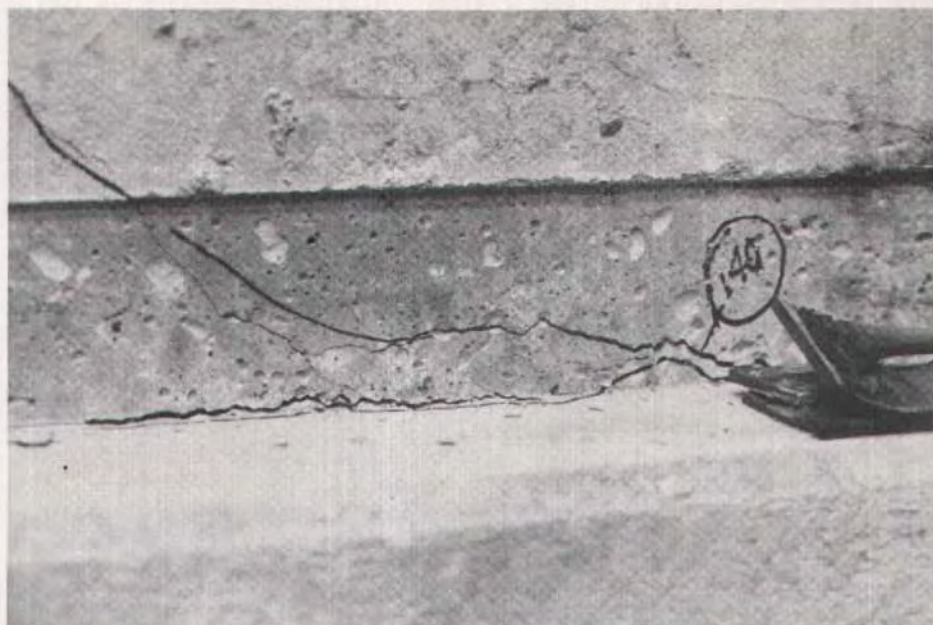


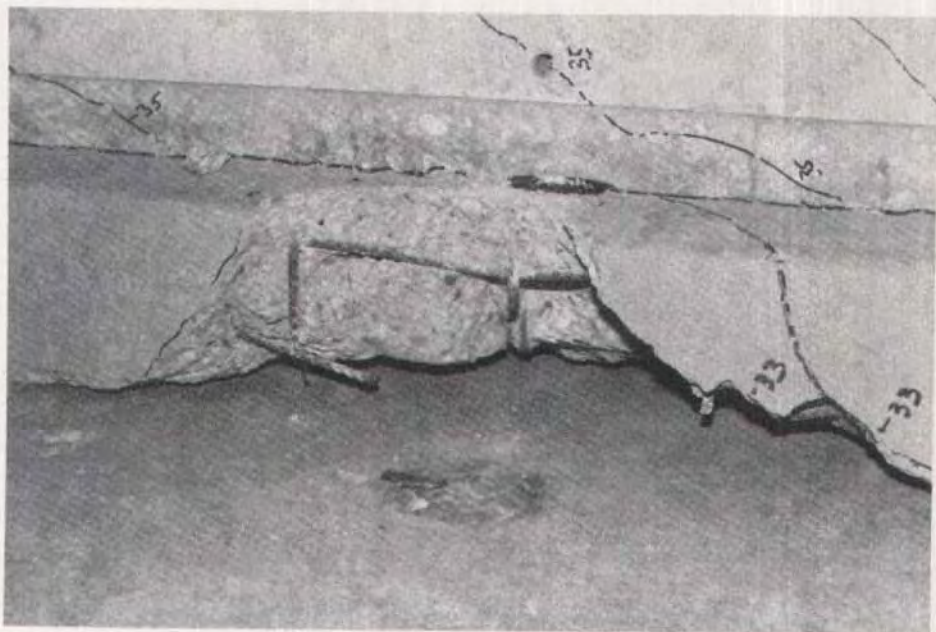
Fig. 19. Crack at ledge/web junction (Specimen 1).



Fig. 20. Crack at ledge/web junction (Specimen 2).



(a) Tee stem at left support.



(b) Sixth tee stem from left.

Fig. 21. Punching shear failures (Specimen 2).



(a) Front.



(b) Back.

Fig. 22. Shear failure (Specimen 3, Phase 1).

recorded strains. Strain in the ledge flexure reinforcement remains low at factored loads because there are no vertical cracks at the ledge/web junction. Despite early cracking at the dapped-end connection, strain levels at factored loads are well below yield strain.

At the maximum test load, the strain in the ledge hanger bars in Specimen 1 are well into the strain hardening range. The ledge hanger bars in Specimen 2

are approaching the yield strain. (Using the 0.2 percent offset method, the yield strain of the #3 bars is about 0.5 percent.) The hanger reinforcing bars at the pocket on Specimen 3 are also near the yield strain. It should be noted that these strains would exceed the nominal yield strain of a Grade 60 bar. Strain in the ledge flexure reinforcement remains low at maximum test load, indicating the absence of ledge flexure cracks.

6. ANALYSIS AND DISCUSSION

General Design Consideration

Location of Critical Section — The shear failure of Specimen 3, shown in Fig. 22, confirms the possibility of an inclined failure plane which carries all of the loads acting on the spandrel. The

crack patterns which occurred in Specimens 1 and 2 suggest a similar possibility. Therefore, the shear and torsion design of spandrel beams should consider a critical section at the face of the support. In addition, the transverse reinforcement spacing required for

shear and torsion at a particular section along the beam should be continued for a distance d inside that section.

An alternate approach is to provide separate hanger reinforcement to transfer the ledge loads to the top of the section and design the spandrel as a directly loaded beam. However, the former approach is more rational because it directly relates to the potential failure planes.

Influence of Deck Connections — As illustrated in Fig. 11, the connections to deck elements do not substantially reduce torsion. The only significant effect of the deck connections is the restraint on lateral displacement induced by bending about the weak principal axis.

Flexure

With regard to flexure, both the strength and serviceability related behavior of the test specimens was satisfactory. It is worth mentioning, however, that flexural cracking of the L-beams only showed up on the back face. This observation is attributed to bending about the weak principal axis.

Shear and Torsion

Prestressed L-Beams — Specimens 1 and 2 were tested at load levels roughly equal to the predicted capacity based on the Zia-Hsu equations, which was the basis for their design. There was no evidence that the negative bending capacity required by compression field theory was needed. As discussed later, some level of positive bending capacity at the face of the support is required.

Pocket Spandrels — The premature shear failure through the full section of the pocket spandrel near the dapped connection is attributed to poor anchorage of the primary flexural reinforcement at the bottom corner of the beam. It may have helped to extend the dapped-end flexural reinforcement beyond the inclined crack; this reinforce-

ment, however, is not very efficient in a deep dap.

Recent research under PCIFSRAD Project No. 6 emphasizes the importance of anchoring the primary flexural reinforcement at dapped connections. This research concludes that the reaction should be limited to the shear strength of the web (the lesser of V_{ci} and V_{cw}), because the primary flexural reinforcement is typically not anchored at the bottom corner of the beam.

Predicting the strength of the concrete section is complicated by the pockets. Hanson¹⁵ found that a conservative prediction of the strength of concrete joists with square openings, but without stirrup reinforcement, was obtained by calculating the load at which cracking at the corner of the opening develops, assuming the shear is distributed in proportion to the area of the section above and below the opening.

One approach to calculating this load is to substitute $b_w(d - h_p)$ for $b_w d$ in ACI Code equations for the shear strength of the concrete section [Eqs. (11-3) or (11-6) for nonprestressed spandrels, or Eqs. (11-10), (11-11) or (11-13) for prestressed spandrels], where h_p is the height of the pocket. Similarly, the strength provided by the shear reinforcement, V_s , is given by:

$$V_s = \frac{A_v f_y (d - h_p)}{s} \quad (4)$$

which reflects an unfavorable crack pattern through the pocket region.

The above approach is believed to be conservative for pocket spandrels, but is not universally applicable to beams with square openings. Using ACI Code Eq. (11-13) and substituting $b_w(d - h_p)$ for $b_w d$, the predicted shear strength provided by the concrete section of Specimen 3 is 110 kips or 93 kips, depending on whether or not the prestress is considered to contribute to shear strength. These predictions are comparable to the failure load of 101 kips.

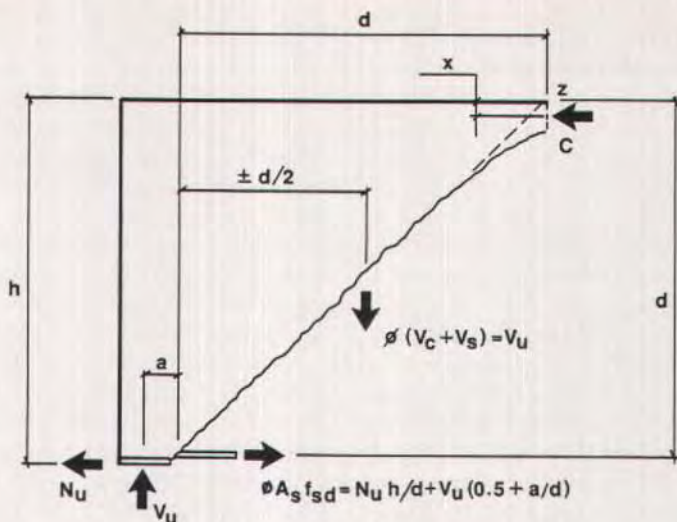


Fig. 23. Forces acting on free body cut off by diagonal tension cracks at support.

It is common practice not to use a deep pocket for the tee stem nearest the support. A welded bracket or Cazaly hanger is used instead. In these cases, the h_p term need not be included for design of the end region.

Detailing Practices — The torsional response of deep spandrels is dominated by out-of-plane bending. There was no evidence of spalling of the side cover which can occur in compact sections subjected primarily to torsion. The use of lapped-splice stirrups in lieu of closed stirrups did not appear to have any detrimental effect, and the absence of hooks on the longitudinal reinforcement did not lead to any apparent problems.

It is unlikely that there would have been any improvement in shear strength of the pocket spandrel had the wire mesh been anchored by a bend at the longitudinal reinforcement. The failure is attributed to poor anchorage of the primary flexural reinforcement, and there was no sign of an anchorage failure of the wire fabric.

Beam End Design

Torsion Equilibrium Reinforcement — The applied torsional load on Specimens 1 and 2 was beyond the predicted capacity of the torsion equilibrium reinforcement required by Eq. (1). To some extent eccentric bearing may have helped equilibrate the applied torsional load. Nonetheless, the test results support the contention that reinforcement for the torsion equilibrium reaction need not be added to the reinforcement for internal torsion.

Longitudinal Reinforcement at End — The premature failure near the dapped connection points out a possible deficiency in the end region of spandrel beams. Fig. 23 shows the forces acting on a free body cut off by diagonal tension cracks at the support. Neglecting the distance from the top of the beam to the compressive force, the developed force required at the face of the support is given by:

$$\phi A_s f_{sd} = N_u h/d + V_u (0.5 + a/d) \quad (5)$$

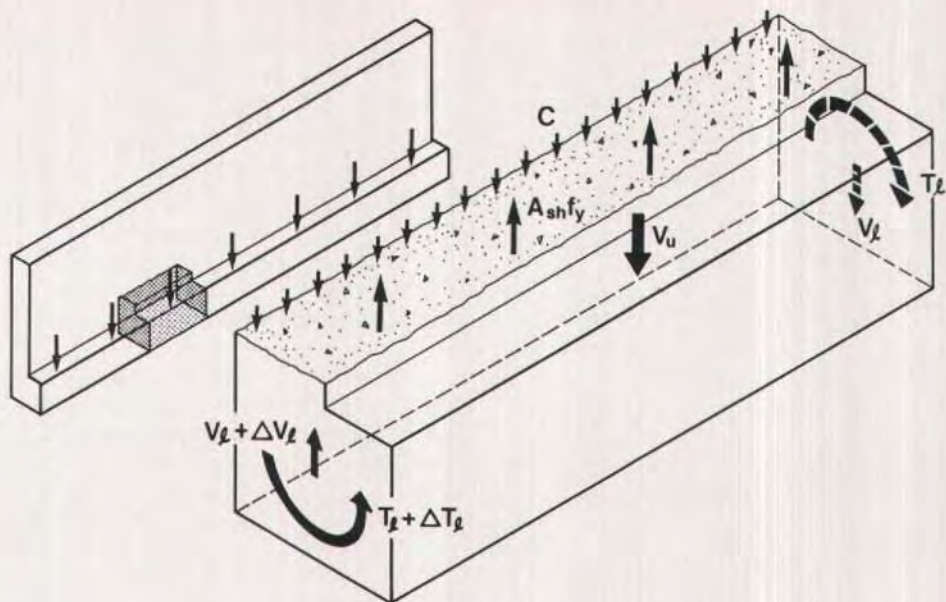


Fig. 24. Transverse forces acting on free body of ledge.

where f_{sd} is the developed stress in the longitudinal reinforcement at the face of the support. The remaining notation is defined in Fig. 23.

For a dapped spandrel, a similar check of the free body forces across an inclined crack through the full section is recommended. Typical cases are included in the design examples in Appendix C.

Beam Ledges

Hanger Reinforcement — The load tests and analytical studies indicate that the eccentricity of the ledge load cannot be neglected in the design of hanger reinforcement. Nonetheless, not all of the load acting on the ledge is suspended from the web, and the effective eccentricity of the ledge load is significantly reduced due to torsion within the ledge. Design by Eq. (2) may be somewhat unconservative, while use of Eq. (3) may be overly conservative.

A design procedure for hanger reinforcement has been developed based on the transverse forces acting on the free body shown in Fig. 24. Summation of moments about the outside face of the spandrel gives:

$$A_{sh} = \frac{V_u(d+a) - \Delta V_l b_l / 2 - \Delta T_l}{\phi f_y d} \quad (6)$$

where

ΔV_l = shear in ledge [Eq. (7)]

ΔT_l = torsion in ledge [Eq. (8)]

b_l = width of ledge measured along bottom of beam

ϕ = strength reduction factor = 0.85

Most of the notation used for hanger reinforcement design is graphically defined in Fig. 25. Similar to Eq. (1), the use of $\phi = 0.85$ instead of 0.9 compensates for the ratio of internal moment arm to total effective depth.

The finite element model study verified that the shear in the ledge, ΔV_l ,

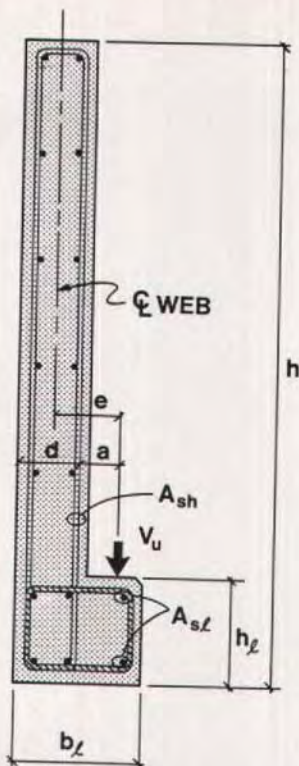


Fig. 25. Notation for hanger reinforcement design.

depends on the internal shear stress distribution, which is calculated by integrating VQ/I from the top of the ledge to the bottom of the beam. In lieu of an exact solution, the following expression, based on the parabolic shear stress distribution in a rectangular beam, gives a conservative approximation of ΔT_t :

$$\Delta T_t = V_u (3 - 2h_l/h) (h_l/h)^2 \quad (7)$$

where

h = overall height of beam

h_l = height of ledge

Observe that ΔT_t depends on the torsional strength of the ledge compared to the total torsional strength of the beam. Accordingly:

$$\Delta T_t = V_u e \gamma_t \frac{(x^2 y)_{ledge}}{\Sigma x^2 y} \quad (8)$$

where

e = distance between applied load and centerline of web

x = shorter overall dimension of rectangular part of cross section

y = longer overall dimension of rectangular part of cross section

$(x^2 y)_{ledge} = b_l h_l^2$ or $b_l^2 h_l$, whichever is smaller

The use of γ_t in Eq. (8) is intended to avoid assigning too much torsion to the ledge. If closed stirrups are provided in the ledge $\gamma_t = 1.0$; otherwise:

$$\gamma_t = \frac{T_c}{T_u} \leq 1 \quad (9)$$

where

T_c = torsional moment strength provided by concrete

T_u = factored torsional moment at critical section

Finally, if the end of the L-beam is dapped, the end reaction will not equilibrate V_l and T_l . Therefore, for dapped-end beams, the total hanger reinforcement is given by:

$$\Sigma A_{sh} = \frac{\Sigma V_u (d + a)}{\phi f_y d} \quad (10)$$

For the L-beams included in this study, Eq. (6) would require about 30 to 60 percent more hanger reinforcement than Eq. (2), depending on γ_t . As previously noted, the use of Eq. (3) doubles the hanger reinforcement requirements compared to Eq. (2). Hanger reinforcement is not additive to shear and torsion reinforcement.

The background research revealed that at least four load tests of spandrel beams were conducted by precast producers several years ago. During two of these load tests, the ledge of an L-beam separated from the web. A more detailed discussion of these prior tests is provided in Project No. 5 report,¹⁶ which is published separately. Similar to the test

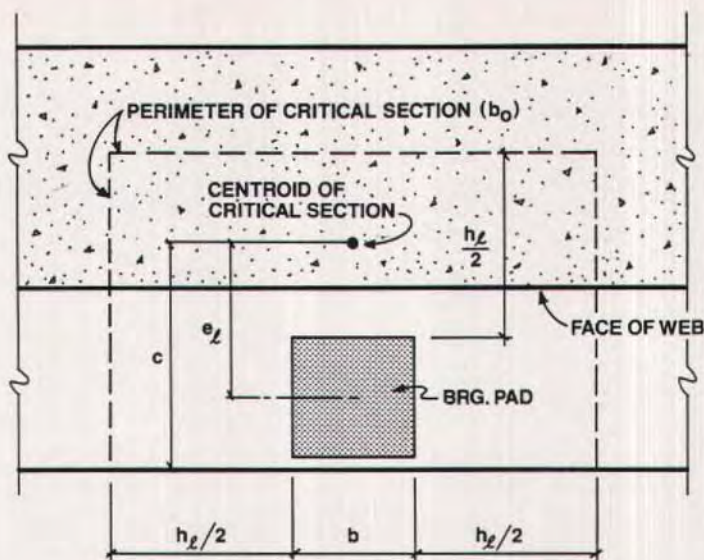


Fig. 26. Plan view of ledge showing eccentricity of ledge load relative to critical section.

of Specimen 1, in these prior load tests a wide horizontal crack developed at the ledge/web junction. In each case, the test was stopped before the ledge actually fell off. All tests indicated the ledge-to-web connection was very ductile despite very light hanger reinforcement. The behavior of these test specimens suggests that due to strain hardening, forces in the hanger reinforcement approaching the ultimate tensile strength can be developed. The ultimate ledge loads, calculated using Eq. (6), are comparable to the maximum test loads.

The reinforcement ratio (A_{sh}/sd , where s is the ledge load spacing) of these spandrels and Specimen 1 was roughly $100f_y$. This amount is similar to the minimum requirement for structural slabs. Because of the ductility demonstrated in these tests, a minimum reinforcement ratio of $100f_y$ is recommended for hanger reinforcement. The effective distribution width for hanger reinforcement is discussed later.

Ledge Punching Shear — The most

unexpected result of the load tests was the early punching shear failures in the ledge of Specimen 2. As discussed in the background section, other researchers have found that the PCI equations for ledge punching shear may be unconservative. One reason may be that the PCI equations do not fully account for the eccentricity between the applied load and the centroid of the critical section. This eccentricity is shown in Fig. 26.

The analysis approach used to investigate transfer of unbalanced moment between slabs and columns can be adapted to punching shear of beam ledges. The shear stress at the inside edge of the ledge is given by:

$$v_c = \frac{V_u}{b_o h_l} + \frac{V_u e_l c}{J_c} \leq 4 \sqrt{f'_c} \quad (11)$$

where

- b_o = perimeter of critical section
- e_l = distance between ledge load and centroid of critical section
- c = distance between centroid of

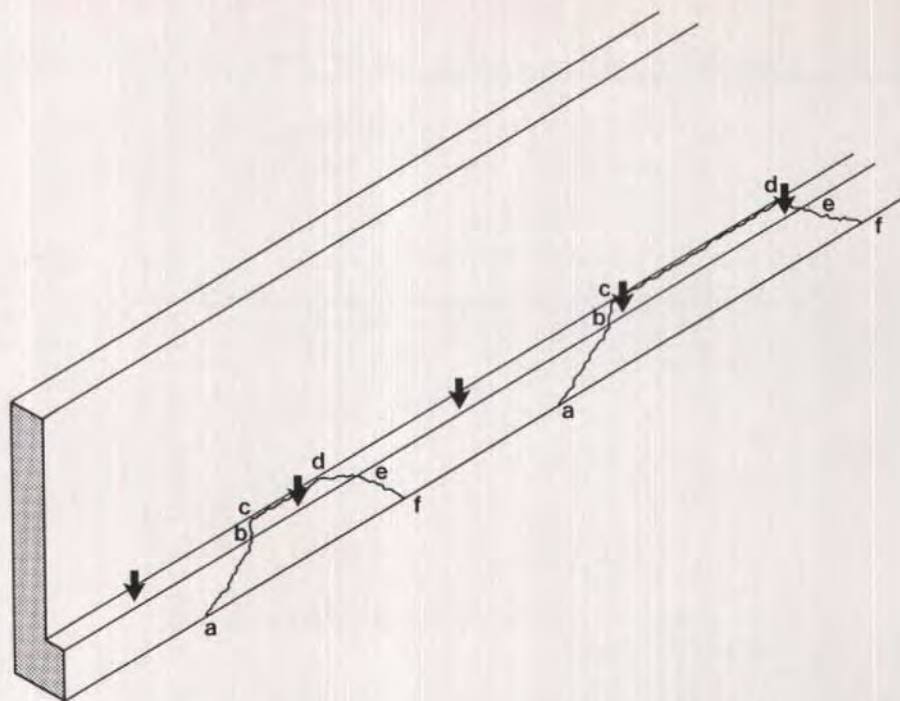


Fig. 27. Local failures related to punching shear strength of ledge.

critical section and inside face of ledge

J_c = property of critical section analogous to polar moment of inertia (see Ref. 17)

This formula assumes that the full height of the ledge is effective and none of the eccentricity is resisted by ledge flexure. The computed punching shear capacity of Specimen 2 using Eq. (11) is 40.5 kips, which is comparable to the failure load of 42.7 kips. Punching shear capacity can be improved by increasing the ledge projection or depth. The use of developed ledge flexure reinforcement should also increase punching shear capacity.

Eq. (11) cannot be accurately applied to conditions where flexural reinforcement developed across the critical section can help resist eccentricity. Also, shear and tensile stresses acting on the full section may reduce the punching

shear resistance of the ledge. However, this study provides evidence that the PCI design equations may be unconservative in some situations, and further research is recommended.

Distribution of Ledge Reinforcement

— Prior to cracking, the L-beam specimens showed evidence of higher stresses in the ledge hanger and flexure reinforcement in the vicinity of the applied load. The finite element model showed a similar concentration of stress. However, the hanger reinforcement strain was much more evenly distributed after the horizontal crack at the ledge/web junction had fully developed. As the ledge separated from the web along the entire length of Specimen 1, it was clear that all of the hanger reinforcement between ledge loads was effective. Ledge flexural cracks did not develop, so nothing was learned about the post-cracking distribution of strain

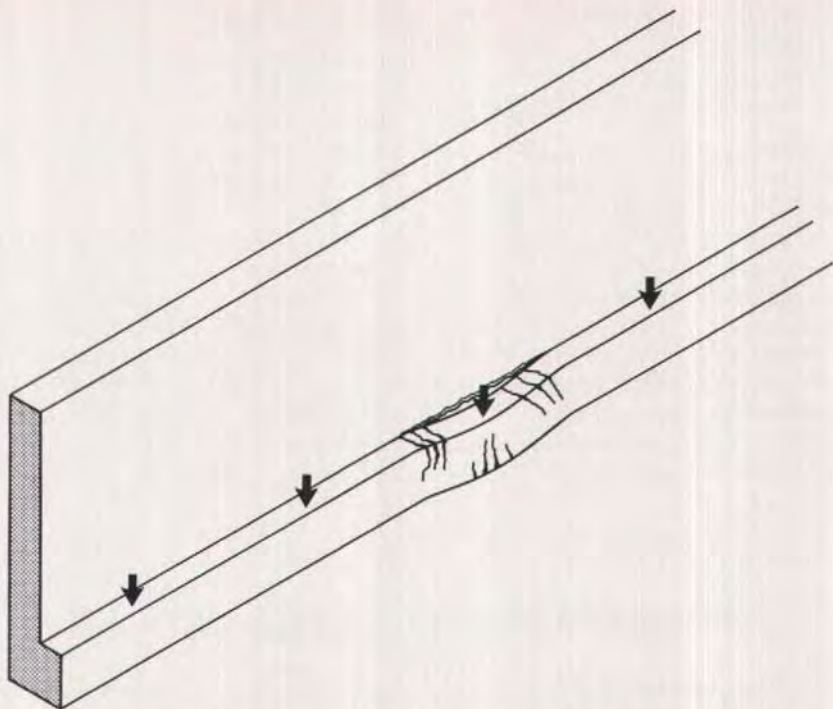


Fig. 28. Local hanger reinforcement failure related to bending strength of ledge.

in ledge flexure reinforcement.

Of course, these results are only applicable to L-beams with geometry and reinforcement similar to the test specimens. Local ledge failures are conceivable, particularly if the loads or load spacing are not uniform. Fig. 27 shows two local failures in which the ledge flexure or hanger reinforcement assumed to resist each ledge load is not fully effective. However, the shear and torsional strength across the inclined failure planes abc and def contribute to the strength.

Note that this contribution is related to the punching shear strength of the ledge. Even though the ledge reinforcement and shear strength may not be fully additive, premature failures of the type shown in Fig. 27 are unlikely. On the other hand, if the reinforcement at the ledge load is required to supplement the punching shear strength, the ledge

flexural reinforcement and hanger reinforcement should also be concentrated at the ledge load.

Fig. 28 shows a local separation between the ledge and web related to the bending strength of the ledge. Assuming the hanger reinforcement stress is evenly distributed between ledge loads (and neglecting ΔV_l) the upward force between loads is equal to V_u/s , where V_u is the stem reaction and s is the ledge load spacing. The corresponding sum of the negative and positive bending moments in the ledge is equal to $V_u s/8$. The reinforcement required to resist this bending moment is given by:

$$A_{st} = \frac{V_u s}{8 \phi d f_y} \quad (12)$$

where

A_{st} = ledge reinforcement in top or bottom of ledge in addition to

reinforcement required for primary moment

d_t = effective depth of A_{st}

ϕ = strength reduction factor = 0.85

Once again, use of a strength reduction factor equal to 0.85 instead of 0.9 compensates for the ratio of internal moment arm to total effective depth.

In summary, this research suggests that all of the hanger reinforcement or ledge flexure reinforcement between ledge loads can be considered effective providing the punching shear and longitudinal bending strength [Eq. (12)] of the ledge are adequate. Further testing should be carried out to verify this assertion.

Beam Pockets

During Phase 2 of the Specimen 3 test, the concrete below one of the beam pockets punched out at a load of 47.6 kips. The predicted failure load based on yielding of the hanger reinforcement is 30.8 kips. The difference is apparently due to a punching shear strength contribution. Based on Eq. (11), the predicted punching shear strength is 31.1 kips per stem. Fully developed inclined cracks below the pocket were observed at tee stem loads of 25 kips. These results indicate that the strength contributions from hanger reinforcement and punching shear are not fully additive.

7. FINDINGS AND RECOMMENDATIONS

The following paragraphs describe the findings based on the background research, analytical studies, and load tests described herein.

● **Critical Section** — Because spandrel beams are loaded near the bottom, a critical section for shear and torsion at the face of the support should be considered.

● **Influence of Deck Connections** — Connections to deck elements do not substantially reduce torsion, however, they are effective in restraining lateral displacement induced by bending about the weak principal axis.

● **Shear and Torsion of Prestressed L-Beams** — Methods which consider a concrete contribution for shear and torsion design of prestressed spandrels, such as the Zia-McGee or the Zia-Hsu methods, have been verified by two tests. Design methods based on compression field theory are somewhat more conservative, particularly with regard to the requirement for negative bending strength at the face of the support.

● **Shear Strength of Pocket Spandrels**

— An approach for considering the effect of the pocket on the shear strength of pocket spandrels has been proposed. While the accuracy of this approach has not been fully verified by tests, it is believed to be conservative.

● **Detailing Practices** — The torsional response of deep spandrels is dominated by out-of-plane bending. The use of lapped-splice stirrups and longitudinal reinforcing bars without hooks does not appear to have any detrimental effect.

● **Beam End Design** — Two independent design checks in the end region of spandrels are recommended. First, reinforcement should be provided to resist out-of-plane bending caused by the horizontal torsional equilibrium reactions. This reinforcement is not additive to the reinforcement for internal torsion, and very little supplemental steel will be required provided a critical section for shear and torsion at the face of the support is considered. Second, the developed force in the primary longitudinal reinforcement at the face of the support, or bottom corner of a dapped-end

connection, should equilibrate the applied normal force, as well as the axial force induced by the vertical reaction.

● **Ledge Hanger Reinforcing** — The eccentricity of the ledge load cannot be neglected in design of hanger reinforcement for ledge-to-web attachment. Nonetheless, not all of the load acting on the ledge is suspended from the web and the effective eccentricity of the ledge load is significantly reduced due to torsion within the ledge. A design procedure which considers these effects has been recommended. Load tests conducted under this program and by others have verified this procedure. In addition, it was determined that hanger reinforcement is not additive to shear and torsion reinforcement. Minimum hanger reinforcement amounts are recommended and distribution of ledge reinforcement is discussed.

● **Ledge Punching Shear** — PCI design equations for the punching shear strength of beam ledges may be unconservative. Further research in this area is recommended.

In closing, it should be re-emphasized that this study has focused on spandrel beams as load-carrying components. In this regard, the research has gone a long way toward the understanding and resolution of several fundamental aspects of spandrel beam design. The findings generally apply to both prestressed and nonprestressed reinforced spandrels commonly used in buildings and parking structures. However, forces from frame action, volume change, handling and vehicular impact were not discussed, and the report does not fully address tolerances, corrosion protection or connection details. These factors must also be carefully considered during the design process.

ACKNOWLEDGMENTS

Throughout the study, the Steering Committee for PCISFRAD Project No. 5 provided helpful guidance and perspective. In particular, Ned Cleland, Alex Aswad, and Kamal Chaudhari contributed significantly through their constructive comments.

The support of Wiss, Janney, Elstner Associates, Inc. in conducting this research is gratefully acknowledged. The author would like to specifically thank John Hanson, John Fraczek, Lilia Glikin, Dirk Heidbrink, and Doris Nelson for their assistance.

The test specimens were fabricated

by J. W. Peters & Sons, Inc. of Burlington, Wisconsin. Their performance in this difficult and precise task is a credit to their talent as a precast producer.

Also, the author wishes to express his appreciation to Susan Klein of Susan Klein Graphic Design for her help in preparing the graphic figures.

Finally, this research was funded by the PCI Specially Funded Research and Development Program. The author wishes to thank the administrators and contributors to that program who made this research possible.

NOTE: Discussion of this paper is invited. Please submit your comments to PCI Headquarters by May 1, 1987.

REFERENCES

1. MacGregor, James G. (Chairman), "The Shear Strength of Reinforced Concrete Members," by the Task Committee on Masonry and Reinforced Concrete of the Structural Division," *Journal of the Structural Division*, ASCE, V. 99, No. ST6, Proceedings Paper 9791, June 1973, pp. 1091-1187.
2. *PCI Design Handbook — Precast and Prestressed Concrete*, Third Edition, Prestressed Concrete Institute, Chicago, Illinois, 1985.
3. *Notes on ACI 318-83*, Fourth Edition, Portland Cement Association, Skokie, Illinois, 1984, pp. 14-28.
4. ACI Committee 318, "Building Code Requirements for Reinforced Concrete (ACI 318-83)," American Concrete Institute, Detroit, Michigan, 1983.
5. Cleland, Ned M., "Identification of Secondary Behavior in Combined Bending, Shear, and Torsion of Reinforced Concrete Ledger Beams," PhD Dissertation, University of Virginia School of Engineering and Applied Science, August 1984. See also "Behavior of Precast Reinforced Concrete Ledger Beams," by Cleland, Ned M., and Baber, Thomas T., *PCI JOURNAL*, V. 31, No. 2, March-April 1986, pp. 96-117.
6. Iverson, James K., and Pfeifer, Donald W., "Bearing Pads for Precast Concrete Buildings," *PCI JOURNAL*, V. 30, No. 5, September-October 1985, pp. 128-154.
7. Zia, Paul and McGee, W. Denis, "Torsion Design of Prestressed Concrete," *PCI JOURNAL*, V. 19, No. 2, March-April 1974, pp. 46-65.
8. *PCI Design Handbook — Precast and Prestressed Concrete*, Second Edition, Prestressed Concrete Institute, Chicago, Illinois, 1978.
9. Zia, Paul and Hsu, Thomas, "Design for Torsion and Shear in Prestressed Concrete," Preprint 3424, ASCE Chicago Exposition, October 1978.
10. Rath, Charles H., "Spandrel Beam Behavior and Design," *PCI JOURNAL*, V. 29, No. 2, March-April 1984, pp. 62-131.
11. Collins, Michael P., and Mitchell, Denis, "Shear and Torsion Design of Prestressed and Non-Prestressed Concrete Beams," *PCI JOURNAL*, V. 25, No. 5, September-October 1980, pp. 85-86.
12. Mirza, Sher Ali, and Furlong, Richard W., "Serviceability Behavior and Failure Mechanisms of Concrete Inverted T-Beam Bridge Bentcaps," *ACI Journal*, Proceedings V. 80, No. 4, July-August 1983, pp. 294-304.
13. Mirza, S. A., and Furlong, R. W., "Design of Reinforced and Prestressed Concrete Inverted T Beams for Bridge Structures," *PCI JOURNAL*, V. 30, No. 4, July-August 1985, pp. 112-137. See also Discussion of Ref. 13 by Basile G. Rabbat and S. A. Mirza and R. W. Furlong in *PCI JOURNAL*, V. 31, No. 3, May-June 1986, pp. 157-163.
14. Krauklis, A. T., and Guedelhofe, O. C., Discussion of "Spandrel Beam Behavior and Design" (Ref. 10), *PCI JOURNAL*, V. 30, No. 5, September-October 1985, pp. 171-174.
15. Hanson, John M., "Square Openings in Webs of Continuous Joists," *PCA Research and Development Bulletin*, Portland Cement Association, Skokie, Illinois, 1969, 14 pp.
16. Klein, Gary J., "Design of Spandrel Beams," PCISFRAD Project No. 5, Prestressed Concrete Institute, Chicago, Illinois, 1986, 100 pp.
17. Rice, Paul F., et al, *Structural Design Guide to the ACI Building Code*, Third Edition, Van Nostrand Reinhold Co., Inc., New York, N.Y., 1985, 477 pp.

* * *

APPENDIX A—NOTATION

<p>a = shear span, distance between concentrated load or reaction and hanger reinforcement</p> <p>A_s = area of flexural tension reinforcement</p> <p>A_{sh} = area of hanger reinforcement</p> <p>A_{sl} = area of reinforcement in top or bottom of ledge in addition to reinforcement required for primary moment</p> <p>A_p = area of shear reinforcement</p> <p>A_{vlt} = area of longitudinal web reinforcement for bending due to torsional equilibrium reactions</p> <p>A_{vve} = area of vertical web reinforcement for bending due to torsional equilibrium reactions</p> <p>b = bearing width of concentrated ledge load</p> <p>b_l = width of ledge measured along bottom of beam</p> <p>b_o = perimeter of critical section</p> <p>b_w = web width</p> <p>c = distance from extreme fiber to neutral axis</p> <p>d = distance from extreme compression fiber to centroid of flexural tension reinforcement</p> <p>d_l = effective depth of ledge reinforcement</p> <p>e = distance from centerline web to ledge load</p> <p>e_l = distance from centroid of critical section for shear to ledge load</p> <p>f'_c = compressive strength of concrete</p> <p>$\sqrt{f'_c}$ = square root of compressive strength of concrete</p> <p>f_{sd} = developed stress in primary flexural reinforcement</p>	<p>f_y = yield strength of nonprestressed reinforcement</p> <p>f_u = ultimate tensile strength of reinforcement</p> <p>h = overall height of section</p> <p>h_l = height of ledge</p> <p>h_p = height of pocket in pocket spandrel</p> <p>h_s = height of beam effective in resisting bending due to torsional equilibrium reactions</p> <p>j = ratio of internal moment arm to total effective depth</p> <p>J_c = property of critical section analogous to polar moment of inertia</p> <p>N_u = axial force at bearing</p> <p>s = spacing of shear or torsion reinforcing</p> <p>s = spacing of ledge loads</p> <p>T_c = torsional moment strength provided by concrete</p> <p>T_l = torsional moment in ledge</p> <p>T_u = factored torsional moment at critical section</p> <p>V_c = shear strength provided by concrete</p> <p>V_l = shear in ledge</p> <p>V_u = factored shear force</p> <p>V_u = factored reaction</p> <p>x = shorter overall dimension of rectangular cross section</p> <p>y = longer overall dimension of rectangular cross section</p> <p>Δ = symbol for difference</p> <p>γ_t = reduction factor for torsion in ledge</p> <p>ϕ = capacity reduction factor</p> <p>Σ = summation symbol</p>
---	---

APPENDIX B — SPANDREL DESIGN CHECKLIST

The following checklist items are presented in an order of their usual consideration in the design process of spandrel beams. Note that these items are not necessarily given in their order of importance. Some of these design considerations are illustrated in Appendix C; however, due to the limited scope of research under PCISFRAD Project No. 5, many of the items listed below are not addressed. The reader is directed to the appropriate section of the PCI Design Handbook and Ref. 10 for discussion of design considerations outside the scope of this research.

Dimensions

- Span
- Web height and width
- Ledge depth and projection
- Daps and blockouts

Loads

- Dead and live
- Frame action
- Volume change
- Vehicular impact

Flexure

- Service load stresses:
 - At release
 - In service
- Flexural strength
- Minimum reinforcement
- Out-of-plane bending:
 - During handling
 - During erection

— Due to vehicular impact

- Sweep due to strand eccentricity
- Principal axis analysis for slender L-beams

Shear and Torsion

- Eccentricity contributing to torsion
- Minimum and maximum torsion
- Transverse reinforcement
- Longitudinal reinforcement

Beam End Design

- Torsion equilibrium reinforcement
- Longitudinal reinforcement at end
- Beam bearing design
- Dapped end design

Ledge Design

- Tee stem bearing
- Punching shear:
 - At interior reaction
 - At outside reaction
- Ledge flexure
- Hanger reinforcement
- Ledge distribution reinforcement

Details

- Column and deck connections
- Reinforcement details:
 - Anchorage/development
 - Spacing
 - Tolerance and clearance
- Corrosion protection:
 - Concrete cover
 - Protection of exposed plates
 - Protection of end of strand
- Inserts for handling

* * *

APPENDIX C — DESIGN EXAMPLES

To illustrate the proposed design procedure of spandrel beams, two design examples are presented. Example 1 covers an L-beam while Example 2 treats a pocket spandrel. Both examples pertain to a parking structure but the basic principles apply to other types of structures.

EXAMPLE 1 — L-BEAM FOR PARKING STRUCTURE

Design Loads

Stem reactions

Dead load (90 psf) =

$$0.09 (60/2) 4 = 10.8 \text{ kips}$$

Live load (50 psf) =

$$0.05 (60/2) 4 = 6.0 \text{ kips}$$

Total service load = 16.8 kips

Factored load = $1.4 \times 10.8 + 1.7 \times 6.0$
= 25.3 kips

Equivalent uniform load

Service: $w = 16.8/4 + 0.675$
= 4.88 kips/ft

Factored: $w_u = 25.3/4 + 1.4 \times 0.675$
= 7.27 kips/ft

The basic uniform loads are increased by the ratio of grid span to design span.

Grid span = 28.0 ft

Shear span = 27.0 ft

Service (adjusted):

$$w = 4.88 \times 28/27 = 5.06 \text{ kips/ft}$$

Factored (adjusted):

$$w_u = 7.27 \times 28/27 = 7.54 \text{ kips/ft}$$

Flexure

The following is a summary of the flexure design. Refer to Section 4.2 of the PCI Design Handbook for details of the design procedure.

Service load moment = 5533 in.-kips

Note: The moment computed using the adjusted equivalent uniform load is about 2 percent greater than the value computed using concentrated loads.

Prestress: Four 1/2-in. diameter strand,

$y_{ps} = 5.0$ in.

At release (7 percent loss)

	f_b	f_t
Computed (psi)	483	-215
Allowable (psi)	2100	-355

In service (17 percent loss)

	f_b	f_t	f_{pc}	f_{pe}
Computed (psi)	166	525	148	430
Allowable (psi)	-424	2250		

Ultimate strength:

$$A_{ps} = 0.612 \text{ in.}^2$$

$$A_s = \text{Four \#4 bars} = 0.80 \text{ in.}^2$$

$$\phi M_n = 9243 \text{ (prestress) plus } 2654 \text{ (mild steel reinforcement) } = 11,897 \text{ in.-kips}$$

$$M_u = 8245 \text{ in.-kips} < 11,897 \text{ in.-kips}$$

$$1.2 M_{cr} = 1.2 (7.5 \sqrt{f'_c + f_{pe}}) Z_b$$

$$= 1.2 (7.5 \sqrt{5000 + 430})$$

$$9406/1000$$

$$= 10,840 \text{ in.-kips} < 11,897 \text{ in.-kips}$$

Refer to Fig. C1 for the L-beam geometry and design data.

Shear and Torsion

The shear and torsion design follows the Zia-Hsu method.⁹ See Fig. C2 for the bending, shear and torsion diagrams.

Shear and torsion properties of section:

Element	x	y	x^2y
Web (above ledge)	8	60	3840
Ledge	12	14	2016
			$\Sigma x^2y = 5856$

$$b_w d = 8 \times 66.6 = 533 \text{ in.}^2$$

$$C_t = b_w d / \Sigma x^2y$$

$$= 5353/5856$$

$$= 0.091 \text{ in.}^{-1}$$

Minimum torsion

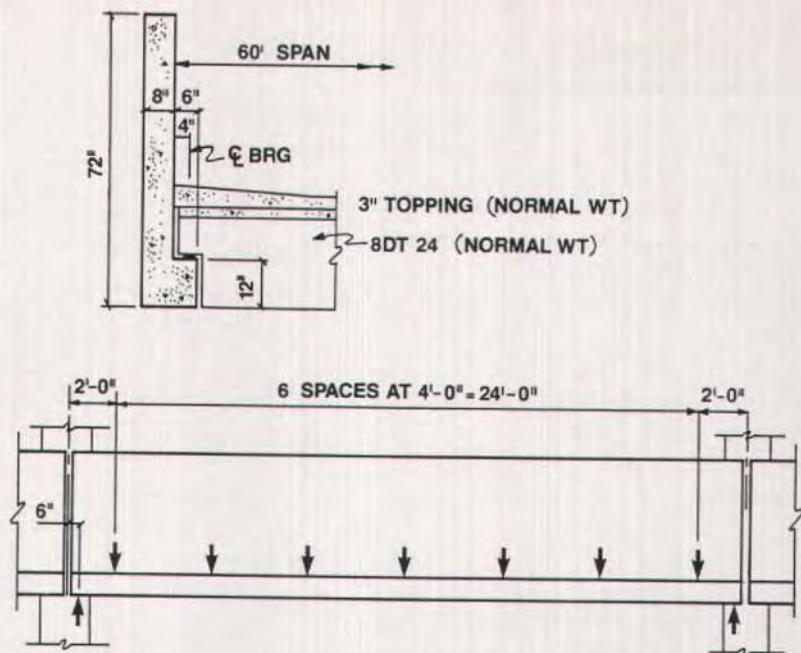
$$\gamma_t = \frac{\sqrt{1 + 10 f_{pc}' / f'_c}}{\sqrt{1 + 10 \times 148 / 5000}}$$

$$= 1.14$$

$$T_{min} = \phi (0.5 \sqrt{f'_c} \gamma_t \Sigma x^2y)$$

$$= 0.85 (0.5 \sqrt{5000} \times 1.14 \times 5856)$$

$$= 201 \text{ in.-kips} < 708 \text{ in.-kips.}$$



DESIGN DATA

$f'_c = 5000$ psi
$f'_{c1} = 3500$ psi
$f_y = 60$ ksi
$f_{pu} = 270$ ksi
($\frac{1}{2}$ in. diameter stress-relieved strand)
clearance to stirrups = $1\frac{1}{4}$ in.

SECTION PROPERTIES

$A = 648$ in. ²
$I = 307,296$ in. ⁴
$y = 32.67$ in.
$Z_b = 9406$ in. ³
$Z_t = 7813$ in. ³
weight = 0.675 kips/ft

Fig. C1. L-beam geometry and design data.

Therefore, torsion design is required.

Maximum torsion

$$C = 12 - 10(f_{pc}/f'_c)$$

$$= 12 - 10(148/5000)$$

$$= 11.7$$

$$T_{max} = \frac{(1/3)C \gamma_t \sqrt{f'_c} \sum x^2 y}{\sqrt{1 + (C \gamma_t V_u / 30 C_t T_u)}}$$

$$= \frac{(1/3)11.7 \times 1.14 \sqrt{5000} \times 5856}{\sqrt{1 + (11.7 \times 1.14 \times 101.8) / (30 \times 0.091 \times 708)}}$$

$$= 1540 \text{ in.-kips} > 708 \text{ in.-kips (ok)}$$

Shear and torsion strength of concrete

At support:

$$V'_c = V_{cw} = (3.5 \sqrt{f'_c} + 0.3 f_{pc}) b_w d + V_p$$

$$= (3.5 \sqrt{5000} + 0.3 \times 0) 8 \times 66.8 + 0$$

$$= 131,900 \text{ lbs} = 131.9 \text{ kips} < V_{ci}$$

Note: Strand is not developed at support, therefore, $f_{pc} = 0$ and $\gamma_t = 1.0$.

$$T'_c = 2 \sqrt{f'_c} \sum x^2 y (\gamma_t - 0.6)$$

$$= 2 \sqrt{5000} \times 5856 (1.0 - 0.6)$$

$$= 331,000 \text{ in.-lbs} = 331 \text{ in.-kips}$$

$$V_c = V'_c / \sqrt{1 + [(V'_c T_u) / (T'_c V_u)]^2}$$

$$= 131.9 / \sqrt{1 + [(131.9 \times 708) / (331 \times 101.8)]^2}$$

$$= 44.8 \text{ kips}$$

$$T_c = T'_c / \sqrt{1 + [(T'_c V_u) / (V'_c T_u)]^2}$$

$$= 331 / \sqrt{1 + [(331 \times 101.8) / (131.9 \times 708)]^2}$$

$$= 311 \text{ in.-kips}$$

At quarter point:

$$M_{cr} = Z_b (6 \sqrt{f'_c} + f_{pc})$$

$$= 9406 (6 \sqrt{5000} + 430) / 1000$$

$$= 8035 \text{ in.-kips}$$

$$V'_c = V_{ci} = 0.6 \sqrt{f'_c} b_w d + V_u M_{cr} / M_u$$

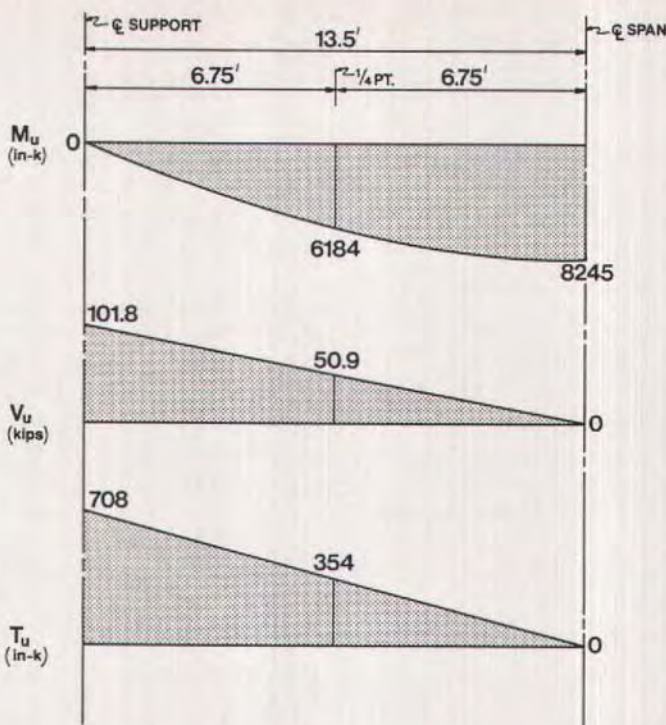


Fig. C2. Moment, shear and torsion diagrams.

$$= 0.6 \sqrt{5000 \times 8 \times 66.6 / 1000} + 50.9 \times 8035 / 6184$$

$$= 88.7 \text{ in.-kips}$$

$$T'_c = 2 \sqrt{5000 \times 5856 (1.14 - 0.6) / 1000} = 447 \text{ in.-kips}$$

$$V_c = 88.7 / \sqrt{1 + [(88.7 \times 354) / (447 \times 50.9)]^2} = 52.0 \text{ in.-kips}$$

$$T_c = 447 / \sqrt{1 + [(447 \times 50.9) / (88.7 \times 354)]^2} = 362 \text{ in.-kips}$$

Transverse reinforcement

At support:

$$A_v/s = (V_u/\phi - V_c)/df_y = (101.8/0.85 - 44.8)/(66.6 \times 60) = 0.019 \text{ in.}^2/\text{in.} = 0.23 \text{ in.}^2/\text{ft}$$

$$T_s = T_u/\phi - T_c = 708/0.85 - 311 = 522 \text{ in.-kips}$$

$$\alpha_t = 0.66 + 0.33 y_1/x_1 \leq 1.5 = 0.66 + 0.33 \times 69/5 = 5.2$$

Therefore, $\alpha_t = 1.5$.

$$A_t/s = T_s/\alpha_t x_1 y_1 f_y$$

$$= 522 / (1.5 \times 5 \times 69 \times 60) = 0.017 \text{ in.}^2/\text{in.} = 0.20 \text{ in.}^2/\text{ft}$$

$$(A_v + 2A_t)/s = 0.23 + 2 \times 0.20 = 0.63 \text{ in.}^2/\text{ft}$$

$$\begin{aligned} \text{Min } (A_v + 2A_t)/s &= 50(b_w/f_y)(1 + 12f_{pc}/f'_c) \leq 200 b_w/f_y \\ &= 50(8/60,000)(1 + 12 \times 148/5000) \\ &= 0.009 \text{ in.}^2/\text{in.} = 0.11 \text{ in.}^2/\text{ft} \end{aligned}$$

See "Beam End Design" for selection of reinforcement.

At quarter point:

$$A_v/s = (50.9/0.85 - 52.0)/(66.6 \times 60) = 0.002 \text{ in.}^2 = 0.02 \text{ in.}^2/\text{ft}$$

$$T_s = 354/0.85 - 362 = 54 \text{ in.-kips}$$

$$A_t/s = 54 / (1.5 \times 5 \times 69 \times 60) = 0.002 \text{ in.}^2/\text{in.} = 0.02 \text{ in.}^2/\text{ft}$$

$$(A_v + 2A_t)/s = 0.02 + 2 \times 0.02 = 0.06 \text{ in.}^2/\text{ft}$$

$$\text{Min } (A_v + 2A_t)/s = 0.11 \text{ in.}^2/\text{ft} \text{ (controls)}$$

Use #3 bars at 12 in.; 0.11 in.²/ft.

Longitudinal reinforcement

$$A_t = (2A_t/s)(x_1 + y_1) \quad \text{Ref. 9, Eq. (7)}$$

Summary of the required transverse and longitudinal reinforcement.

Location	$2A_t/s$ (in. ² /in.)	A_t [Eq. (7)] (in. ²)	T_u (in.-kips)	V_u (kips)	A_t [Eq. (8)] (in. ²)	A_t (in. ²)
At support	0.034	2.52	708	101.8	0.05	2.52
At quarter point	0.002	0.15	354	50.9	1.90	1.90

or

$$A_t = \left[\frac{440x}{f_y} \frac{T_u}{T_u + V_u/3C_t} - \frac{2A_t}{s} \right] (x_1 + y_1)$$

Ref. 9, Eq. (8)

whichever is greater, where:

$$2A_t/s \text{ [in Eq. (8)]} \geq 50b_w (1 + 12f_{pc}/f'_c)/f_y$$

$$= 0.009 \text{ in.}^2/\text{in.}$$

A summary of the required transverse and longitudinal reinforcement of the L-beam at the support and quarter point is given above.

Use seven #4 bars each side of the web; $A_t = 2.80 \text{ in.}^2$

Beam End Design

Torsion equilibrium reinforcement

$$d_s = 8 - 1.25 - 0.5 = 6.25 \text{ in.}$$

$$h_s = 72 - 12 - 6 = 54 \text{ in.}$$

$$A_{wt} = A_{wt} =$$

$$\frac{T_u}{2\phi f_y d_s} = \frac{708}{2 \times 0.85 \times 60 \times 6.25} = 1.11 \text{ in.}^2$$

$$A_{wt}/h_s = 1.11/54 = 0.021 \text{ in.}^2/\text{in.} = 0.25 \text{ in.}^2/\text{ft}$$

$A_t/s = 0.20 \text{ in.}^2/\text{ft}$ (see transverse reinforcement calculated previously).

Therefore,

A_{wt}/s controls.

$$(A_v + 2A_{wt})/s = 0.23 + 2 \times 0.25 = 0.76 \text{ in.}^2/\text{ft}$$

Use #4 stirrups at 6 in. = 0.80 in.²/ft. Six #4 bars in web above ledge;

$$A_{wt} = 1.20 \text{ in.}^2 > 1.11 \text{ in.}^2$$

Therefore, the specified longitudinal reinforcement is adequate.

Reinforced concrete bearing

Based on Section 6.9 of the PCI Design Handbook, $A_{vt} + A_n = 1.02 \text{ in.}^2$ Use two #7 bars welded to the bearing plate. Again, refer to the Handbook for details of the design procedure.

Longitudinal reinforcement at end

$$N_u = 0.2V_u = 0.2 \times 101.8 = 20.4 \text{ kips}$$

$$a = 5 + (h - d) = 5 + (72 - 66.6) = 10.4 \text{ in.}$$

$$\phi A_s f_{sd} = N_u h/d + V_u (0.5 + a/d)$$

$$= 20.4 \times 72/66.6 + 101.8(0.5 + 10.4/66.6)$$

$$= 88.9 \text{ kips}$$

Summarized at the top of the next page are the developed stresses and forces of the provided reinforcement.

Ledge Design

Bearing, punching shear and ledge flexure

The following is a summary of the ledge design following the PCI Design Handbook procedures (refer to Part 6 of the Handbook).

Bearing: Bearing reinforcement is not required.

Punching shear: Punching shear strength is about twice the 25.3-kip stem reaction. Note that the apparent inaccuracy of the PCI equations here is not a concern. Also, the 42.7 kip test result is much greater than the stem reaction.

Ledge flexure: $A_s = 0.50 \text{ in.}^2$ distributed evenly between stem reactions. Use #4 bars at 12 in.; $A_s = 0.80 \text{ in.}^2$

Hanger reinforcement

$$V_u = 25.3 \text{ kips}$$

$$\Delta V_t = V_u (3 - 2h_t/h) (h_t/h)^2$$

$$= 25.3(3 - 2 \times 12/72) (12/72)^2$$

$$= 1.9 \text{ kips}$$

$$\gamma_t = T_c/T_u = 311/708 = 0.44$$

$$\Delta T_t = V_u e \gamma_t (x^2 y)_{\text{ledge}} / \Sigma x^2 y$$

$$= 25.3 \times 8 \times 0.44 \times 2016/5856$$

$$= 30.7 \text{ in.-kips}$$

$$d = 8 - 1.25 - 0.25 = 6.5 \text{ in.}$$

$$a = 4 + 1.25 + 0.25 = 5.5 \text{ in.}$$

Summary of the developed stresses and forces of provided reinforcement.

Reinforcement	Developed stress	Developed force
Four #4 bars	$60 \times 8/12 = 40$ ksi	$0.9 \times 40 \times 0.8 = 28.8$ kips
Four 1/2 in. diameter strand	$150 \times 10/25 = 60$ ksi	$0.9 \times 60 \times 0.61 = 32.9$ kips
Two #7 bars (welded to bearing plate)	60 ksi	$0.9 \times 60 \times 1.20 = 64.8$ kips
		126.5 kips (ok)

Summary of the required transverse reinforcement.

Parameter	Formula	Near support	Midspan
Shear/torsion	$(0.5A_v + A_t)/s$	0.32	0.11 (min)
Torsion equilibrium	$(0.5A_v + A_{sv})/s$	0.38	—
Hanger reinforcement Provided	A_{sh} (per ft)	0.26 #4 bars at 6 in. (0.40)	0.20 #3 bars at 6 in. (0.22)

$$\begin{aligned}
 A_{sh} &= [V_u(d+a) - \Delta V_l b_l/2 - \Delta T_l]/(\phi f_y d) \\
 &= [25.3(6.5+5.5) - 1.9 \times 14/2 - 30.7]/0.85 \times 60 \times 6.5 \\
 &= 0.78 \text{ in.}^2
 \end{aligned}$$

Near support use #4 stirrups at 6 in., 3 ft tributary length at end reaction.

$$A_{sh} = 0.4 \text{ in.}^2/\text{ft} (3 \text{ ft}) = 1.20 \text{ in.}^2$$

Midspan: Add #3 L-bars at 12 in.; alternate with #3 stirrups at 12 in.

$$A_{sh} = 2 \times 0.11 \times 4 = 0.88 \text{ in.}^2$$

$$\begin{aligned}
 \text{Minimum: } A_{sh} &= 100 s d / f_y \\
 &= 100 \times 48 \times 6.5 / 60,000 \\
 &= 0.52 \text{ in.}^2
 \end{aligned}$$

A summary of the transverse reinforcement (inside face, in.²/ft) is given above.

Ledge distribution reinforcement

Punching shear strength is adequate. Therefore, all hanger reinforcement and ledge flexure reinforcement between ledge loads are considered effective, provided the flexural strength of the ledge is adequate.

$$d_l = 12 - 3 = 9 \text{ in.}$$

$$\begin{aligned}
 A_{sl} &= V_u s / 8 \phi d_l f_y \\
 &= 25.3 \times 48 / (8 \times 0.85 \times 9 \times 60) \\
 &= 0.33 \text{ in.}^2
 \end{aligned}$$

The two #4 bars at the end of the ledge are not required for the basic flexural moment. However, the bars are needed to help resist $1.2M_{cr}$. Therefore, they may be considered as A_{sl} reinforcement.

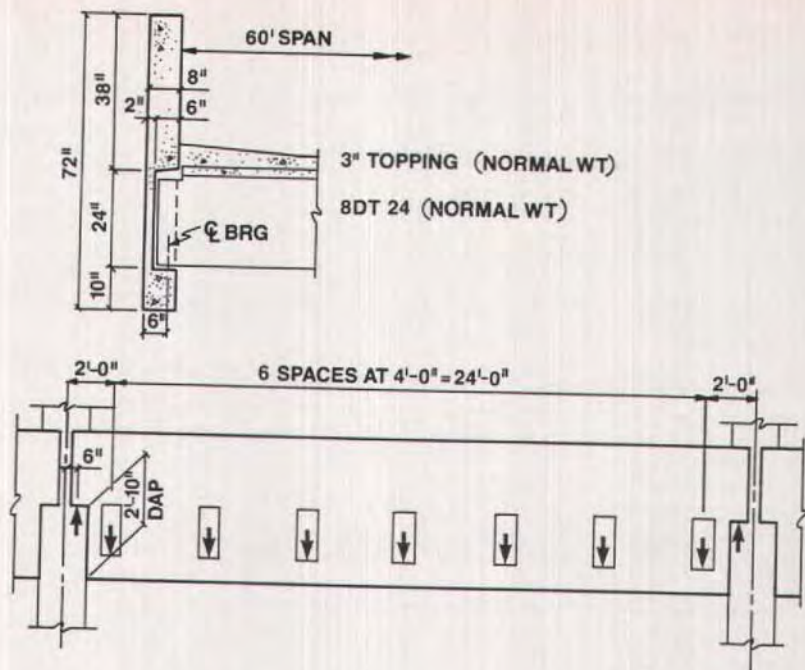
EXAMPLE 2 — POCKET SPANDREL FOR PARKING STRUCTURE

This example illustrates the design of shear, end region, and hanger reinforcement for a dapped pocket spandrel. Note that the pocket is provided near the dapped end. Often this pocket is omitted due to detailing difficulties. A welded bracket or Cazaly hanger is used instead.

Shear and bending forces are identical to those used in Example 1 (Fig. C2). Refer to Fig. C3 for framing details and design data.

In addition, the following is given:

$$\begin{aligned}
 f_{pc} &= 167 \text{ psi} \\
 f_{pe} &= 904 \text{ psi (at pocket)} \\
 d &= 67.0 \text{ in.}
 \end{aligned}$$



DESIGN DATA	FULL SECTION	AT POCKET
$f'_c = 5000$ psi	$A = 576$ in. ²	432 in. ²
$f'_{c1} = 3500$ psi	$I = 248,832$ in. ⁴	204,288 in. ⁴
$f_r = 60$ ksi (bars)	$y_b = 36.0$ in.	40.7 in.
$f_y = 70$ ksi (WWF)	$Z_b = 6912$ in. ³	5023 in. ³
$f_{pu} = 270$ ksi	$Z_t = 6912$ in. ³	6520 in. ³

Fig. C3. Pocket spandrel geometry and design data.

Shear and Torsion

Torsion at support

Stem reaction = 25.3 kips; $e = 2.0$ in.

$$T_u = 7 \times 25.3 \times 2.0 / 2 = 177 \text{ in.-kips}$$

Inside outer reaction:

$$T_u = 5 \times 25.3 \times 2.0 / 2 = 127 \text{ in.-kips}$$

Minimum torsion

$$\gamma_t = \frac{\sqrt{1 + 10f_{pc}/f'_c}}{\sqrt{1 + 10 \times 167 / 5000}} = 1.15$$

$$\Sigma x^2 y = 8^2 \times 72 = 4608$$

$$T_{min} = \phi (0.5 \sqrt{f'_c} \gamma_t \Sigma x^2 y) = 0.85 \times 0.5 \sqrt{5000} \times 1.15 \times 4608 / 1000 = 159 \text{ in.-kips}$$

Therefore, torsion design is not required inside the outer reaction. Design the end region for torsion equilibrium

reactions at the supports.

Shear strength of concrete

At support:

$$V_c = V_{cw} = (3.5 \sqrt{f'_c} + 0.3 f_{pc}) b_w (d - h_p) = (3.5 \sqrt{5000} + 0) 8 (67.0 - 24.0) / 1000 = 85.1 \text{ kips}$$

At quarter point (see Section 11.4.2 of ACI 318-83 Commentary):

$$M_{cr} = Z_b (6 \sqrt{f'_c} + f_{pc}) = 5023 (6 \sqrt{5000} + 904) / 1000 = 6672 \text{ in.-kips (at pocket)}$$

$$V_e = V_{ct} = 0.6 \sqrt{f'_c} b_w (d - h_p) + V_u M_{cr} / M_u = 0.6 \sqrt{5000} \times 8 (67.0 - 24.0) / 1000 + 50.9 \times 6672 / 6184 = 69.5 \text{ kips} < V_u$$

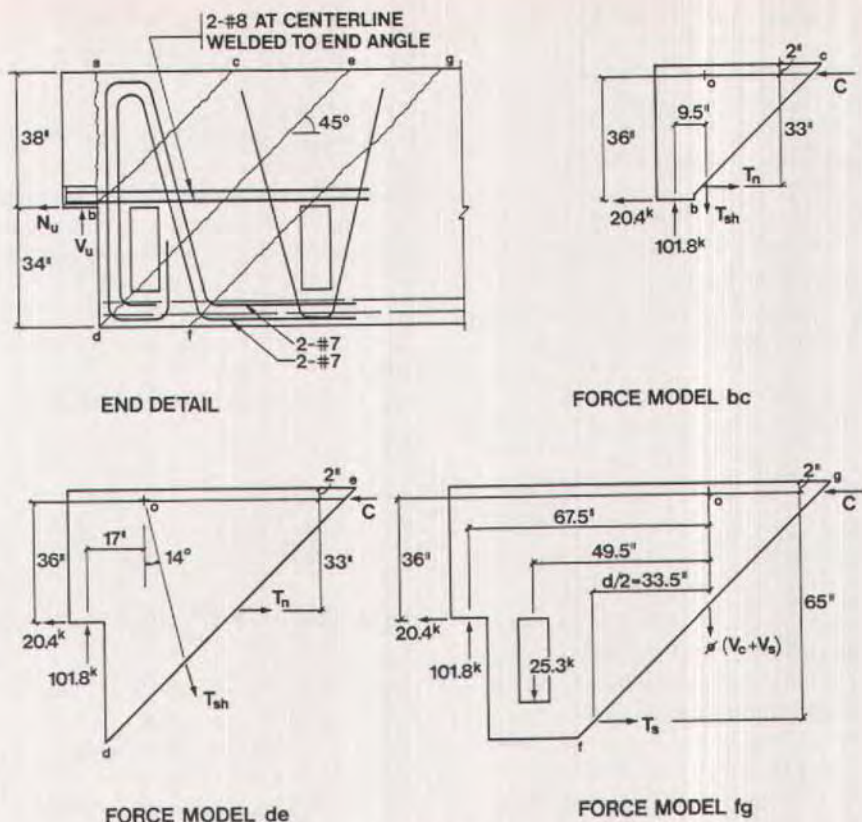


Fig. C4. Dapped end detail and force models.

Shear reinforcement

$$A_v/s = (V_u/\phi - V_c)/(d - h_p)f_y$$

$$= (101.8/0.85 - 85.1)/(67.0 - 24.0)60$$

$$= 0.16 \text{ in.}^2/\text{ft} \text{ or } 0.013 \text{ in.}^2/\text{in.}$$

$$\text{Min } A_v/s = 50b_w/f_y$$

$$= 50 \times 8/60,000 = 0.0067 \text{ in.}^2/\text{in.}$$

$$= 0.080 \text{ in.}^2/\text{ft}$$

Use one layer of 12 x 6 - W2.0 x W4.0 each face, full length.

$$A_v/s = 2 \times 0.08 = 0.16 \text{ in.}^2/\text{ft}$$

Beam End Design

Torsion equilibrium reinforcement

$$d_s = 8.0 - 1.5 = 6.5 \text{ in.}$$

$$A_{wt} = A_{wl} = T_u/2\phi f_y d_s$$

$$= 177/(2 \times 0.85 \times 70 \times 6.5)$$

$$= 0.23 \text{ in.}^2$$

$$h_s = 38 - 6 = 32 \text{ in.}$$

$$A_{wp}/s = A_{wl}/s = 0.23/32$$

$$= 0.0072 \text{ in.}^2/\text{in.}$$

$$= 0.086 \text{ in.}^2/\text{ft}$$

Use an additional layer of 6x6 - W4.0xW4.0 inside face, each end.

$$A_{wp}/s = A_{wl}/s = 0.08 \text{ in.}^2/\text{ft}$$

Dapped end design

Dapped end design is based on the end detail and equilibrium force models shown in Fig. C4. It should be noted, however, that the reinforcement scheme and design procedure have not been validated by load tests.

For direct shear, see Section 6.13.2 of the PCI Design Handbook.

$$\mu_e = 1000 \lambda b h \mu V_u \leq 3.4$$

$$= 1000 \times 1 \times 8 \times 38 \times 1.4 / (101.8 \times 1000)$$

$$= 4.18 > \mu_e = 3.4$$

$$A_n = N_u / (\phi f_y) = 20.4 / (0.85 \times 60) = 0.40 \text{ in.}^2$$

$$A_s = 2V_u / (3\phi f_y \mu_e) + A_n = 2 \times 101.8 / (3 \times 0.85 \times 60 \times 3.4) + 0.40 = 0.79 \text{ in.}^2$$

Two #8 bars provided; $A_s = 1.44 \text{ in.}^2$

$$A_h = 0.5(A_s - A_n) = 0.5(0.72 - 0.40) = 0.16 \text{ in.}^2$$

6x6 - W4.0xW4.0 provided

$$A_h = 3.0 \times 0.08 = 0.24 \text{ in.}^2$$

Crack at re-entrant corner (force model bc): Neglect inclined hanger reinforcement.

$$\Sigma F_v = 0 \rightarrow T_{sh} = V_u = 101.8 \text{ kips}$$

$$A_{sh} = T_{sh} / \phi f_y = 101.8 / (0.85 \times 60) = 2.00 \text{ in.}^2$$

Four #7 bars provided; $A_{sh} = 2.40 \text{ in.}^2$

$$\Sigma M_o = 0 \rightarrow T_n = (20.4 \times 36 + 101.8 \times 9.5) / 33 = 51.6 \text{ kips}$$

$$A_n = T_n / \phi f_y = 51.6 / (0.85 \times 60) = 1.01 \text{ in.}^2$$

Two #8 bars provided; $A_s = 1.44 \text{ in.}^2$

Crack at bottom corner (force model de)

Neglect vertical hanger reinforcement (not effective at bend).

$$\Sigma F_v = 0 \rightarrow T_{sh} = V_u / \cos 14 = 101.8 / \cos 14 = 104.9 \text{ kips}$$

$$A_{sh} = 104.9 / (0.85 \times 60)$$

$$= 2.06 \text{ in.}^2 \text{ (four #7 bars)(ok)}$$

$$\Sigma M_o = 0 \rightarrow T_n = (20.4 \times 36 + 101.8 \times 17) / 33 = 74.7 \text{ kips}$$

$$A_n = 74.7 / (0.85 \times 60)$$

$$= 1.46 \text{ in.}^2 \text{ (two #8 bars)(ok)}$$

Full section (force model fg)

Hanger reinforcement is not effective due to bend. Neglect A_n reinforcement.

$$\Sigma M_o = 0 \rightarrow T_s = (20.4 \times 36 + 101.8 \times 67.5 - 25.3 \times 49.5) / 65 = 97.7 \text{ kips}$$

From PCI Design Handbook Fig.

$$4.10.4, f_{ps} = 170 \text{ ksi.}$$

$$\phi A_{ps} f_{ps} = 0.9 \times 0.61 \times 170 = 93.3 \text{ kips (say ok)}$$

Check depth of compression block

$$a = \Sigma F_n / 0.85 b f'_c = (97.7 - 20.4) / 0.85 \times 8 \times 5 = 2.3 \text{ in.}$$

$$a/2 = 2.3/2 = 1.2 \text{ in.} < 2 \text{ in. (ok)}$$

Hanger Reinforcement

At pocket

$$A_{sh} = V_u \phi f_y = 25.3 / (0.90 \times 60) = 0.47 \text{ in.}^2$$

Use one #4 U-bar (slope of 1 to 4) at each pocket (plus two W4.0 wires).

$$A_{sh} = 2 \times 0.20 (\cos 14) + 2 \times 0.04 = 0.47 \text{ in.}^2$$

$$l_{dn} = 1200 d_b / \sqrt{f'_c} = 1200 \times 0.5 / \sqrt{5000} = 8.5 \text{ in. (ok)}$$

* * *

Metric (SI) Conversion Factors

$$1 \text{ ft} = 0.3048 \text{ m}$$

$$1 \text{ in.} = 25.4 \text{ mm}$$

$$1 \text{ kip} = 4448 \text{ N}$$

$$1 \text{ lb} = 4.448 \text{ N}$$

$$1 \text{ psi} = 0.006895 \text{ MPa}$$

$$1 \text{ ksi} = 6.895 \text{ MPa}$$

$$1 \text{ psf} = 4.882 \text{ kgf/m}^2$$